Title
Investigating the Impact of Simvastatin on Human Gut Bacteria

Author
Escalante, Veronica

Publication Date
2023

Peer reviewed|Thesis/dissertation

Investigating the impact of simvastatin on human gut bacteria

by
Veronica Escalante

DISSERTATION
Submitted in partial satisfaction of the requirements for degree of
DOCTOR OF PHILOSOPHY

in

Biochemistry and Molecular Biology

in the

GRADUATE DIVISION
of the
UNIVERSITY OF CALIFORNIA, SAN FRANCISCO

Approved:

DocuSigned by:
Danica Galonic Fujimori
82967A5AE18B4D6...

Danica Galonic Fujimori
Chair

DocuSigned by:
Peter J. Turnbaugh
[illegible]441...

Peter J. Turnbaugh

DocuSigned by:
Deanna Kroetz
0611A116B51E4AA...

Deanna Kroetz

Committee Members

Dedication

To my family and friends in Mexico and El Paso that inspired me along the way to get to where I am today.

Acknowledgements

I would like to express my deepest gratitude to my Ph.D. advisor, Dr. Peter J. Turnbaugh, for being the best mentor throughout my time at UCSF. Thank you for letting me join your wonderful lab that I have come to call a piece of home and for letting me explore a new field. Your unwavering guidance, insightful feedback, and constant encouragement throughout the journey of this research have been instrumental in shaping the direction and quality of this work.

As I went along my scientific journey, I met a village at UCSF who supported and encouraged me along the way. Thank you to everyone who is now or has been a part of the Turnbaugh lab for always encouraging me to do my best. Your support, discussions, and insights have helped me become both a better person and scientist. Thanks to Drs. Jordan Bisanz, Renuka Nayak and Cecilia Noecker who patiently mentored me in the gut microbiome field and motivated me. Thanks to Ernesto Valencia, Daryll Gempis and Ethel Enoex-Godonoo for going above and beyond to create a welcoming environment. I would also like to thank the Tetrad Graduate Program staff for their support; my collaborators for providing me with the tools and expertise to carry out my research; and my thesis committee – Drs. Danica Fujimori and Deanna Kroetz – for helping me unravel my scientific findings into a story.

I am profoundly indebted to my parents and little sister for their support and understanding. Their encouragement and sacrifices have been the cornerstone of my academic pursuits. My parents for making the sacrifice of crossing the Mexico-US border everyday just so my little sister and I would gain a better education and learn English.

Without their sacrifice, I would not have gone to college and would not be in the Tetrad Ph.D. program at UCSF.

To my husband Emmanuel and my daughter Elena, your unwavering belief in me has been my rock, and your constant encouragement has sustained me through the challenges. You are my anchor and for that I love you. This Ph.D. is also your accomplishment.

Lastly, I extend my gratitude to all those who contributed to this work, directly or indirectly. Your insights and support have enriched this research in ways I could not have accomplished alone.

In writing this thesis, I am reminded that true achievement is the culmination of the efforts of many, and for that, I am truly humbled and thankful.

Contributions

Chapter 2 contains work from a manuscript in revision:

- Escalante V, Nayak RR, Noecker C, Babdor J, Spitzer M, Deutschbauer AM and Turnbaugh PJ. Simvastatin induces human gut bacterial cell surface genes. 2023.

Abstract

Investigating the Impact of Simvastatin on Human Gut Bacteria

Veronica Escalante

Drugs intended to target mammalian cells can have broad off-target effects on the human gut microbiota with potential downstream consequences for drug efficacy and side effect profiles. Yet, despite a rich literature on antibiotic resistance, we still know very little about the mechanisms through which commensal bacteria evade non-antibiotic drugs. Here, we focus on statins, one of the most prescribed drug types in the world and an essential tool in the prevention and treatment of high circulating cholesterol levels. Prior work in humans, mice, and cell culture support an off-target effect of statins on human gut bacteria; however, the genetic determinants of statin sensitivity remain unknown. First, we confirmed that simvastatin inhibits the growth of diverse human gut bacterial strains grown in communities and in pure cultures. Drug sensitivity varied between phyla and was dose dependent. We selected two representative simvastatin-sensitive species for more in-depth analysis: *Eggerthella lenta* (phylum: Actinobacteriota) and *Bacteroides thetaiotaomicron* (phylum: Bacteroidota). Transcriptomics revealed that both bacterial species upregulate genes in response to simvastatin that alter the cell membrane, including fatty acid biogenesis (*E. lenta*) and drug efflux systems (*B. thetaiotaomicron*). Transposon mutagenesis identified a key efflux system in *B. thetaiotaomicron* that enables growth in the presence of simvastatin. Taken together, these results emphasize the importance of the bacterial cell membrane in countering the off-target effects of host-targeted drugs. Continued mechanistic dissection of the various mechanisms through which the human gut microbiota evades drugs will be essential to understand and predict

the effects of drug administration in human cohorts and the potential downstream consequences for health and disease.

Table of Contents

List of Figures

List of Supplementary Figures

Chapter 1: Introduction

1.1 Background

The intricate relationship between pharmaceuticals and the human gut microbiota has come to light through comprehensive population-level surveys, revealing a notable connection with inter-individual variations in gut microbial community structure[1,2]. Remarkably, this connection transcends traditional boundaries, extending from drugs targeting infectious diseases to a diverse range of pharmaceutical interventions aimed at addressing chronic diseases. Pharmaceuticals employed in contexts as varied as cancer treatment[3], management of rheumatoid arthritis[4], and interventions for cardiovascular disease[1,5] have all been implicated in shaping the complex landscape of the gut microbiota. Among these interactions, the influence of statins on the gut microbiome has stood as an intriguing subject.

Statins rank as some of the top pharmaceuticals prescribed for their lipid-lowering capabilities, an important measure in the treatment and prevention of cardiovascular disease[6]. The fascination surrounding statin-gut microbiota interactions arises from the widespread use of statins among patients and the potential for the development of adverse events often unexplained by genetics or other environmental factors[6,7]. Gastrointestinal off-target effects, (bloating, diarrhea, and constipation) and other rare yet severe adverse events (muscle damage and diabetes) are often reported amongst statin users, suggesting that statins may induce alterations of the gut microbiome. The capacity of statins to perturb the composition and function of the gut microbiome holds clinical significance, prompting further investigation into the mechanisms at play. Moreover, recent studies have indicated a broader positive impact of statins on the gut microbiome.

For instance, one study[5] has provided evidence suggesting that statins may reduce the risk of obesity. These observations underscore the urgency of delving into the intricate interplay between statins and the gut microbiome to gain insights into their roles in human health and disease.

The interaction between statins and the gut microbiome finds substantiation in studies conducted on humans, murine models, and cell cultures. Initial investigations in humans have unveiled associations between bile acid metabolites produced by the gut microbiome and statin bioavailability and efficacy[8]. Metagenomic sequencing has recently illuminated connections between the gut microbiome and both statin efficacy and toxicity[9]. The implications of this interaction extend to murine models, suggesting a direct causal link between statins and the gut microbiome[10–14]. Additionally, intriguing insights have emerged regarding the potential role of the gut microbiome in contributing to the lipid-lowering effects of statins[15]. Notably, evidence from the screening of human gut bacterial isolates suggests direct inhibition of bacterial growth by statins[16].

Despite the wealth of evidence highlighting the interaction between statins and gut microbiome, several fundamental questions remain unanswered. Of particular intrigue is the mystery surrounding the bacterial targets of statins, considering that their canonical target, 3-hydroxy-3-methylglutaryl coenzyme A (HMG-CoA) reductase, is seldom found within the human gut microbiome[17]. The limitations of previous *in vitro* studies, which focused solely on a single statin dose in monoculture, underscore the necessity for comprehensive investigations. Along those lines, the questions surrounding the minimal inhibitory concentration (MIC) and the applicability of observed growth inhibition to microbial communities warrant deeper exploration. Furthermore, a comprehensive

understanding of the effects of statins necessitates an exploration of their impact on bacterial physiology, gene expression, and metabolic activity. Moreover, until now, insights into the genes and gene products contributing to bacterial sensitivity to statins, as well as the extent of their prevalence across different bacterial phyla, have remained elusive.

Herein, we undertake a comprehensive analysis of the interactions between a representative statin, simvastatin, and the human gut microbiome both *in vitro*. The selection of simvastatin stems from its clinical relevance and well-documented interactions with the microbiome in humans, mice, and cell cultures. As anticipated, the study unravels the dose-dependent effects of simvastatin on bacterial growth across diverse phyla. Leveraging a combination of transcriptomics and transposon mutagenesis, the work here identifies pathways conducive to growth in response to statins in representative bacterial strains from two distinct phyla—one Gram-positive and one Gram-negative. These findings carry implications that extend beyond statins, offering a conceptual and experimental framework to dissect the impact of a broader array of statins and other drugs on the human gut microbiome.

1.2 References

1. Falony, G., Joossens, M., Vieira-Silva, S., Wang, J., Darzi, Y., Faust, K., Kurilshikov, A., Bonder, M.J., Valles-Colomer, M., Vandeputte, D., et al. (2016). Population-level analysis of gut microbiome variation. Science *352*, 560–564.

2. Zhernakova, A., Kurilshikov, A., Bonder, M.J., Tigchelaar, E.F., Schirmer, M., Vatanen, T., Mujagic, Z., Vila, A.V., Falony, G., Vieira-Silva, S., et al. (2016). Population-based metagenomics analysis reveals markers for gut microbiome composition and diversity. Science *352*, 565–569.

3. Spanogiannopoulos, P., Kyaw, T.S., Guthrie, B.G.H., Bradley, P.H., Lee, J.V., Melamed, J., Malig, Y.N.A., Lam, K.N., Gempis, D., Sandy, M., et al. (2022). Host and gut bacteria share metabolic pathways for anti-cancer drug metabolism. Nat Microbiol *7*, 1605–1620.

4. Nayak, R.R., Alexander, M., Deshpande, I., Stapleton-Gray, K., Rimal, B., Patterson, A.D., Ubeda, C., Scher, J.U., and Turnbaugh, P.J. (2021). Methotrexate impacts conserved pathways in diverse human gut bacteria leading to decreased host immune activation. Cell Host Microbe *29*, 362–377.e11.

5. Vieira-Silva, S., Falony, G., Belda, E., Nielsen, T., Aron-Wisnewsky, J., Chakaroun, R., Forslund, S.K., Assmann, K., Valles-Colomer, M., Nguyen, T.T.D., et al. (2020). Statin therapy is associated with lower prevalence of gut microbiota dysbiosis. Nature *581*, 310–315.

6. Golomb, B.A., and Evans, M.A. (2008). Statin adverse effects: a review of the

literature and evidence for a mitochondrial mechanism. Am. J. Cardiovasc. Drugs *8*, 373–418.

7. Thompson, P.D., Panza, G., Zaleski, A., and Taylor, B. (2016). Statin-Associated Side Effects. J. Am. Coll. Cardiol. *67*, 2395–2410.

8. Kaddurah-Daouk, R., Baillie, R.A., Zhu, H., Zeng, Z.-B., Wiest, M.M., Nguyen, U.T., Wojnoonski, K., Watkins, S.M., Trupp, M., and Krauss, R.M. (2011). Enteric microbiome metabolites correlate with response to simvastatin treatment. PLoS One *6*, e25482.

9. Wilmanski, T., Kornilov, S.A., Diener, C., Conomos, M.P., Lovejoy, J.C., Sebastiani, P., Orwoll, E.S., Hood, L., Price, N.D., Rappaport, N., et al. (2022). Heterogeneity in statin responses explained by variation in the human gut microbiome. Med *3*, 388–405.e6.

10. Catry, E., Pachikian, B.D., Salazar, N., Neyrinck, A.M., Cani, P.D., and Delzenne, N.M. (2015). Ezetimibe and simvastatin modulate gut microbiota and expression of genes related to cholesterol metabolism. Life Sci. *132*, 77–84.

11. Caparrós-Martín, J.A., Lareu, R.R., Ramsay, J.P., Peplies, J., Reen, F.J., Headlam, H.A., Ward, N.C., Croft, K.D., Newsholme, P., Hughes, J.D., et al. (2017). Statin therapy causes gut dysbiosis in mice through a PXR-dependent mechanism. Microbiome *5*, 95.

12. Cheng, T., Li, C., Shen, L., Wang, S., Li, X., Fu, C., Li, T., Liu, B., Gu, Y., Wang, W., et al. (2021). The Intestinal Effect of Atorvastatin: Akkermansia muciniphila and

Barrier Function. Front. Microbiol. *12*, 797062.

13. Zhang, S., Yuan, L., Li, H., Han, L., Jing, W., Wu, X., Ullah, S., Liu, R., Wu, Y., and Xu, J. (2021). The Novel Interplay between Commensal Gut Bacteria and Metabolites in Diet-Induced Hyperlipidemic Rats Treated with Simvastatin. J. Proteome Res. 10.1021/acs.jproteome.1c00252.

14. Xu, M., Luo, L.-L., Du, M.-Y., Tang, L., Zhou, J., Hu, Y., and Mei, H. (2022). Simvastatin Improves Outcomes of Endotoxin-induced Coagulopathy by Regulating Intestinal Microenvironment. Curr Med Sci *42*, 26–38.

15. He, X., Zheng, N., He, J., Liu, C., Feng, J., Jia, W., and Li, H. (2017). Gut Microbiota Modulation Attenuated the Hypolipidemic Effect of Simvastatin in High-Fat/Cholesterol-Diet Fed Mice. J. Proteome Res. *16*, 1900–1910.

16. Maier, L., Pruteanu, M., Kuhn, M., Zeller, G., Telzerow, A., Anderson, E.E., Brochado, A.R., Fernandez, K.C., Dose, H., Mori, H., et al. (2018). Extensive impact of non-antibiotic drugs on human gut bacteria. Nature *555*, 623–628.

17. Gill, S.R., Pop, M., Deboy, R.T., Eckburg, P.B., Turnbaugh, P.J., Samuel, B.S., Gordon, J.I., Relman, D.A., Fraser-Liggett, C.M., and Nelson, K.E. (2006). Metagenomic analysis of the human distal gut microbiome. Science *312*, 1355–1359.

Chapter 2: Simvastatin impacts the growth and response of human gut bacteria.

2.1 Introduction

Population-level surveys of the human gut microbiota have revealed that pharmaceuticals are the top predictor of inter-individual variations in gut microbial community structure[1,2]. Surprisingly, this association extends beyond drugs for infectious disease to drugs used in a wide range of noncommunicable diseases, including cancer[3], rheumatoid arthritis[4], and cardiovascular disease[1,5]. The off-target of statins on the gut microbiota is of particular interest due to the ubiquity of the use of these drugs in patients and the existence of rare but potentially severe adverse effects, including muscle damage and diabetes[6].

Studies in humans, mice, and cell culture support a robust and clinically relevant interaction between statins and the gut microbiota. Early work in humans demonstrated that bile acid metabolites produced by the gut microbiome are positively associated with statin bioavailability and efficacy[7], consistent with a recent metagenomic sequencing study demonstrating that the gut microbiome is associated with both statin efficacy and toxicity[8]. Statins may also have a broader beneficial effect on the gut microbiota; for example, by decreasing the risk of obesity[5]. While gold-standard data from double-blinded longitudinal randomized controlled trials remains lacking, experiments in mouse models support a direct causal effect of statins on the gut microbiota[9–13] and even a potential role of the gut microbiota in contributing to their lipid-lowering effects[14]. Furthermore, a screen of human gut bacterial isolates suggested that statins can directly inhibit the growth of gut bacteria[15].

However, despite the extensive literature supporting an important interaction between statins and the gut microbiome, multiple key questions remain. The bacterial targets of statins remain a mystery, given that their canonical target, 3-hydroxy-3-methylglutaryl coenzyme A (HMG-CoA) reductase, is rarely found in the human gut microbiome[16]. The one prior *in vitro* study[15] only evaluated a single dose of statins in mono-culture; thus, the minimal inhibitory concentration (MIC) and relevance of the observed growth inhibition to microbial communities remain unclear. Furthermore, although growth inhibition is a valuable starting point, far more work is needed to assess the impact of statins on bacterial physiology, gene expression, and metabolic activity. Perhaps most importantly, prior to this study we lacked any insight into the genes and gene products that contribute to bacterial sensitivity to statins or if these mechanisms were shared across phyla.

To address these major knowledge gaps, we conducted an in-depth analysis of the interactions of a single representative statin (simvastatin) and the human gut microbiota. Simvastatin was selected due to its clinical relevance and clear evidence for microbiota interactions in humans[7], mice[10,14], and cell culture[15]. As expected, we found that simvastatin has dose-dependent effects on bacterial growth across phyla. Further, we used a combination of transcriptomics and transposon mutagenesis to identify pathways in representative strains from two bacterial phyla (one Gram-positive and one Gram-negative) that support bacterial growth in the presence of statins. These results emphasize the parallels between pathways for resistance to antibiotics and host-targeted drugs[15], while providing an experimental and conceptual framework to dissect the impact of a broader range of statins or other drugs on human gut bacteria.

2.2 Results

2.2.1 Simvastatin directly inhibits gut bacterial growth in mixed cultures

We used our established methods for the *ex vivo* incubation of the human gut microbiota[4,17] to test the impact of simvastatin on gut microbial community structure in the absence of a host. Stool samples were selected from ImmunoMicrobiome cohort, an ongoing study of the microbiome and immune system of healthy participants. Growth was tracked longitudinally for 48 hours by optical density and 16S rRNA gene sequencing (16S-seq) was performed at the experimental endpoint. The simvastatin concentrations tested (≤25 μg/mL) were below the estimated maximum intestinal concentration (160 μg/mL) even after accounting for absorption in the proximal gut (96 μg/mL in stool).

Simvastatin had a significant impact on the gut microbiota across multiple metrics. Analysis of our growth curves revealed a dose-dependent delay in the overall growth of the human gut microbiota, resulting in a significant increase in the time it took to reach mid-exponential phase (**Figure 2.1**). Community-wide carrying capacity and growth rate trended lower in response to simvastatin but did not reach statistical significance potentially due to insufficient power (**Figure S1**). We also observed a significant and dose-dependent decrease in microbial diversity, as assessed by the Shannon diversity index (**Figure 2.1**) and the number of amplicon sequence variants (ASVs; **Figure S1**). Consistent with prior studies[17], analysis of the full 16S-seq dataset revealed marked inter-individual variations in the gut microbiota with a slight convergence based on simvastatin concentration (**Figure 2.1**). After stratifying the data by subject, we observed clear and statistically significant effects of simvastatin on gut microbial community structure (**Figure 2.1**). At the phylum level, simvastatin significantly decreased Bacteroidota and increased

Verrucomicrobiota (**Figure 2.1**). Significant differences were also apparent at the ASV level, including 7 depleted ASVs and 3 enriched ASVs (**Figure 2.1**). With the exception of an ASV identified as *Eggerthella lenta,* the remaining 6 depleted ASVs were significantly affected at both doses of simvastatin. An ASV identified as *Bacteroides thetaiotaomicron* was the most dramatically depleted ASV, with a 9-fold reduction in abundance. Taken together, these results show that simvastatin has a dramatic effect on the human gut microbiota in the absence of a host.

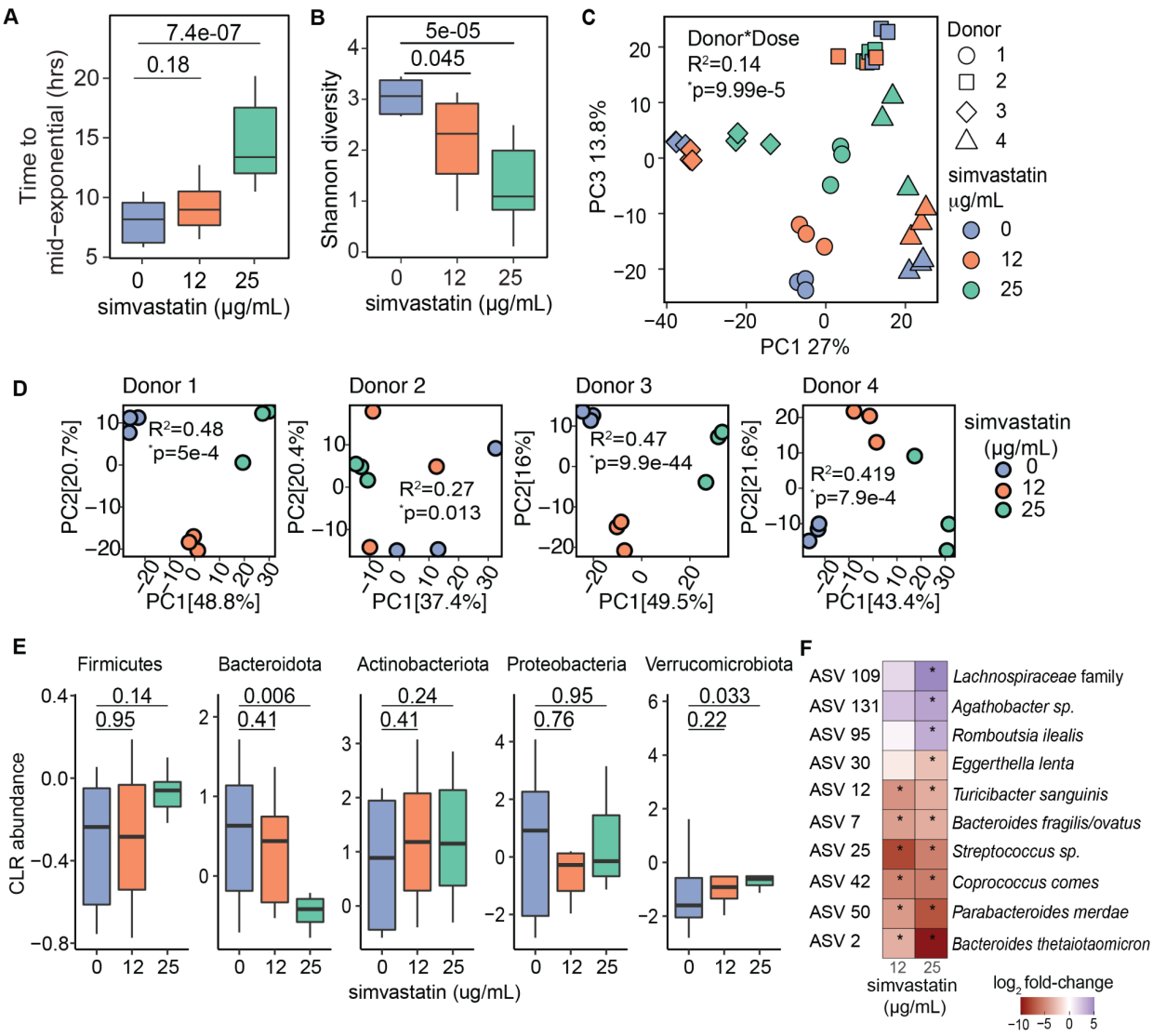

Figure 2.1 Simvastatin directly alters the growth and community structure of the human gut microbiota. Human *ex vivo* stool cultures (n=4 donors, n=3 biological replicates/concentration) were grown with simvastatin or a vehicle control for 48 hours and analyzed by 16S rRNA gene sequencing. (A) Time to mid-exponential growth in hours from the growth data. (B) Bacterial diversity decreases as the concentration of simvastatin increases based on the Shannon diversity index. (C) Principal components 1 and 3 of Euclidean distances using center $\log_2$-ratio (CLR)-transformed values from 16S-seq data colored by simvastatin concentration and shaped by donor sample to facilitate the visualization of their effects. (D) Principal components 1 and 2 of Euclidean distances using CLR-transformed values from 16S-seq data calculated for each donor. (E) Taxonomic data from all samples aggregated at the phylum-level, CLR-transformed and compared across simvastatin concentrations. (figure caption continued on the next page)

(figure caption continued from the previous page) (F) ASVs differentially abundant across all samples in response to simvastatin at 25 μg/mL that also show consistent directionality in response to simvastatin at 12 μg/mL (ALDEx2 comparing samples treated with each simvastatin concentration relative to the vehicle). Colors indicate the difference in CLR-transformed values between simvastatin and vehicle groups; * indicates significance with a nominal p-value<0.05 (Wilcoxon rank test). Boxplots in panels A,E: top and bottom hinges are the first and third quartiles, horizontal lines denote the median, and whiskers extend to the maximum and minimum values. *p*-values represent Wilcoxon rank-sum tests (panels A,B,E) or PERMANOVA tests (panel C and D) between treatment groups.

2.2.2 Simvastatin directly inhibits gut bacterial growth in pure cultures

Next, we sought to gain a more precise understanding of the growth inhibitory properties of simvastatin on human gut bacteria grown in isolation. We leveraged a previously generated collection of 39 human gut bacterial strains spanning 5 phyla[3,4]. Each strain was grown in rich media (brain heart infusion with supplements; BHI^{CHAV}), which we previously showed supports the robust growth of this entire collection[3]. Simvastatin was included at a range of concentrations (1.56-100 μg/mL) at or below the estimated distal gut concentration (96 μg/mL). The majority of the tested strains (29/39) had a measurable MIC (defined by a 90% decrease in carrying capacity), which ranged from 25-100 μg/mL (**Figure 2.2**). Of the strains with a measurable MIC, members of the Firmicutes and Actinobacteriota phyla had a significantly higher MIC relative to members of the Bacteroidota phylum (**Figure S2**). Within the tested Actinobacteriota, simvastatin sensitivity varied >3-fold, with *Collinsella aerofaciens* and *Bifidobacterium longum* tolerating higher levels than *E. lenta* and the other *Coriobacteriaceae*. Of note, both *B. thetaiotaomicron* and *E. lenta* were consistently affected by simvastatin in the context of a complex community and pure cultures. This fact, together with our extensive tools for *B. thetaiotaomicron* genetics[18] and *E. lenta* functional genomics[19] led us to focus on these two bacteria for more in-depth analysis.

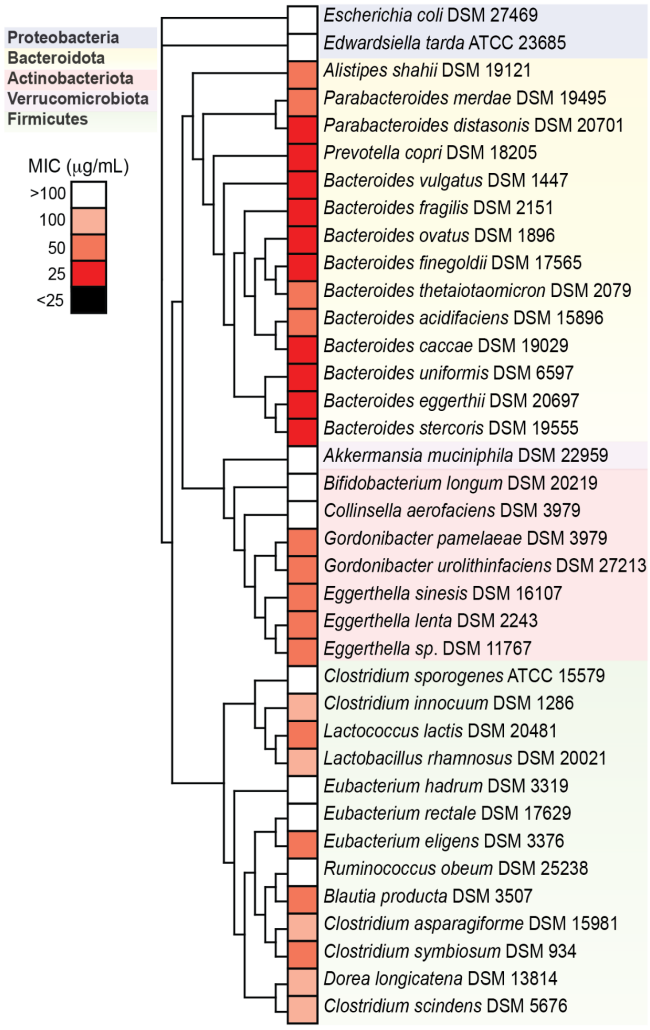

Figure 2.2 Simvastatin directly inhibits the growth of human gut bacterial isolates. A diverse panel of 39 representative gut bacterial strains were incubated with varying concentrations of simvastatin (1.56-100 μg/mL in 2-fold increments, n=3 biological replicates/concentration tested) and the MIC determined. A phylogenetic tree using full-length 16S rRNA gene sequences for each organism was constructed. MIC, minimum inhibitory concentration. The tree shows 37 of the isolates (2 additional *Eggerthella* strains were tested but only one of each species was included in the tree).

2.2.3 *E. lenta* upregulates genes for membrane biogenesis in response to simvastatin

Given the lack of variation in simvastatin sensitivity within the *Eggerthellaceae*, we turned to transcriptional profiling (RNA-seq) to gain insights into the genes and metabolic pathways altered in response to simvastatin. We grew *E. lenta* in rich media and added 3 concentrations of simvastatin [low, med, high; 0.1-1X MIC] or vehicle controls at mid-exponential growth. Samples were collected 15 minutes later and used for RNA-seq and analysis.

Simvastatin induced a substantial change in *E. lenta* gene expression. Principal components analysis revealed clear grouping of the overall transcriptomes of the two higher doses relative to the lowest dose and vehicle controls (**Figure 2.3**). These differences were statistically significant (R^2=0.393 and p=0.046, PERMANOVA; comparing simvastatin doses to vehicle controls). The number of differentially expressed genes (FDR<0.1 and $|\log_2$ fold-change$|$>1, DESeq2) was dose-dependent (**Figure 2.3**), ranging from 2-250 upregulated and 0-240 downregulated genes relative to vehicle controls. At the highest dose ~16% (490/3,086) of *E. lenta* protein-coding genes were differentially expressed. The set of differentially expressed genes was dose-dependent, with 294 genes unique to the highest dose (**Figure 2.3**). Pathway enrichment analysis demonstrated that the two higher doses of simvastatin consistently impacted 7 genes involved in fatty acid biosynthesis important for building lipids used in the cell membrane (**Figure 2.3**).

Interestingly, we observed 4 simvastatin-dependent genes annotated in NCBI as multiple antibiotic resistance transcriptional regulators (MarRs)[20]. MarRs typically repress their own promoter[21,22]. Ligand binding releases MarR from the promoter, inducing

expression of MarR and neighboring genes (**Figure 2.4**). MarR has been implicated in stress responses as well as the degradation/export of phenolic compounds and antibiotics[22]. MarRs can bind to diverse ligands, including the antibiotics kanamycin, salicylate, and 2,4-dinitrophenol[21–24], but direct binding to statins has not been reported.

In total, the *E. lenta* genome contains 9 MarR homologs, of which 4 are upregulated with a high dose of simvastatin. These 4 gene clusters have diverse functions including ATP-binding cassette (ABC) drug transport, heat shock response, fatty acid biosynthesis, and multidrug and toxic compound extrusion (**Figure 2.4**). Of note, one of these putative MarR-regulated clusters encodes 6 genes involved in fatty acid biosynthesis (**Figure 2.4**), all of which are induced at the two higher doses of simvastatin, consistent with our pathway enrichment analysis (**Figure 2.4**). Taken together, these results support a working model in which simvastatin either directly or indirectly affects *E. lenta* MarR, lifting its repression of multiple gene clusters, including a suite of genes that are predicted to alter cell membrane lipid composition. Notably, all of the 9 MarR genes are also conserved across the *E. lenta* species, supporting their core importance for stress response (**Figure S3**).

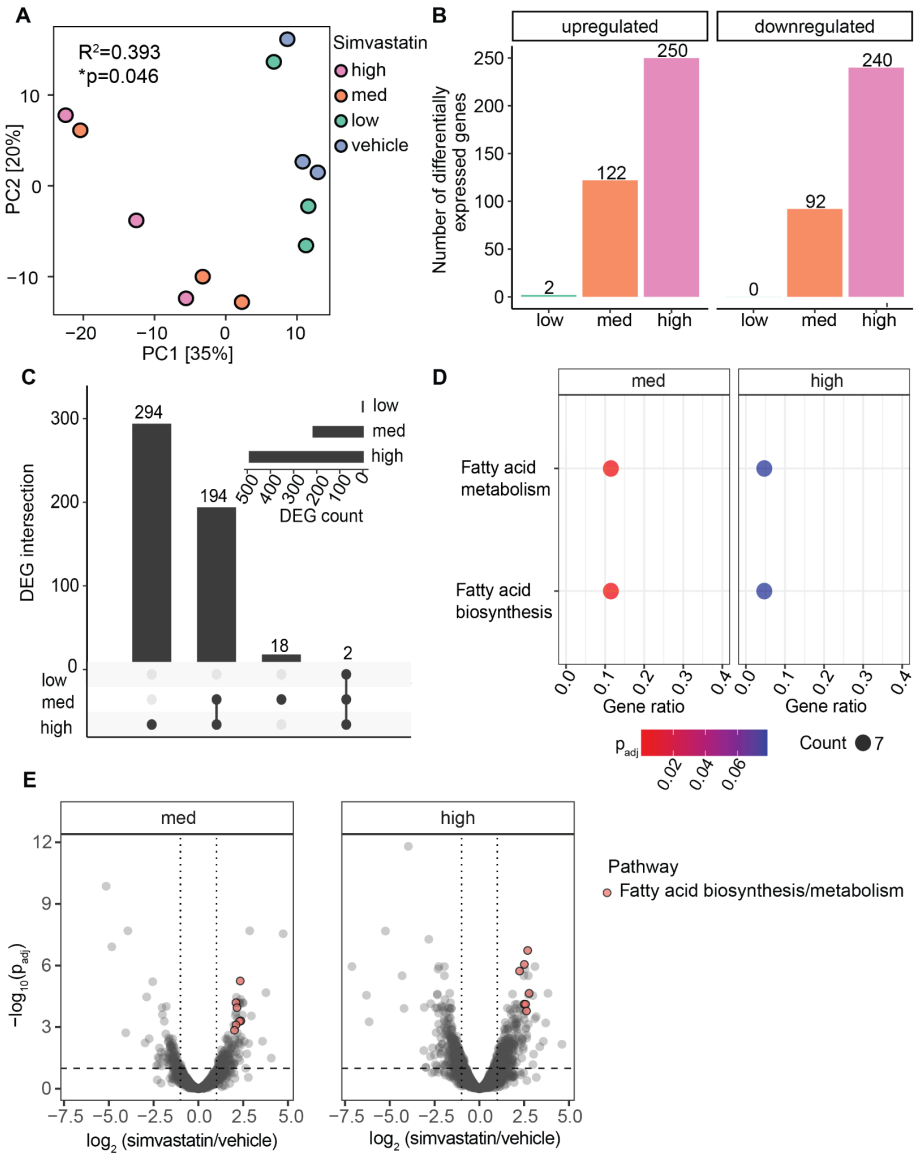

Figure 2.3 Simvastatin has a dose-dependent effect on the *E. lenta* transcriptome and induces genes for cell membrane integrity. (A) PCA of *E. lenta* DSM 2243 RNA-seq data comparing three doses of simvastatin to vehicle controls: low, low-dose (6 µg/mL); med, medium-dose (30 µg/mL); high, high-dose (60 µg/mL). Statistical results of PERMANOVA are reported (n=3 biological replicates/group). (B) Number of differentially expressed genes (DEGs; FDR<0.1 and $|\log_2$ fold-change$|$>1, DESeq2) comparing each simvastatin dose relative to vehicle controls. (C) Overlap between DEGs across simvastatin doses. (D) Volcano plot of the medium and high simvastatin doses relative to vehicle controls: horizontal line, $|\log_2$ fold-change$|$>1; vertical line, FDR<0.1. Colored points represent fatty acid biosynthesis pathway genes found to be significantly enriched by a KEGG pathway enrichment using clusterProfiler (p_{adj}<0.2, Benjamini–Hochberg correction). The KEGG overview map for fatty acid metabolism (KEGG map01212), which the fatty acid biosynthesis pathway falls under, was also significantly enriched due to an overlapping set of genes between them.

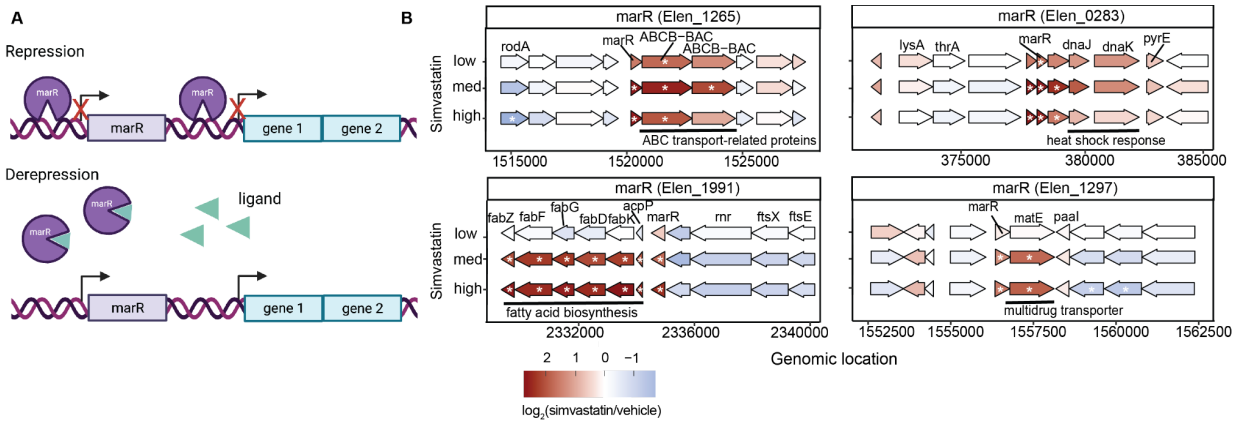

Figure 2.4 Simvastatin induces multiple MarR-dependent gene clusters in *E. lenta*. (A) Diagram of a marR and its mode of gene regulation (created with BioRender.com). MarR acts as a transcriptional repressor of itself and neighboring gene clusters by binding to site-specific DNA regions upstream. When MarR is bound to a ligand, repression is released and allows for the transcription of previously repressed genes[22]. (B) Locus diagram showing 4 of the 9 differentially expressed *marR* genes (FDR<0.1 and $|\log_2$ fold-change$|$>1, DESeq2) and their adjacent gene clusters across different doses of simvastatin. Colors are $\log_2$ fold-changes relative to vehicle controls. Significance is represented with an asterisk. Gene and gene cluster annotations shown where available.

2.2.4 *B. thetaiotaomicron* upregulates efflux systems that protect against simvastatin

Next, we sought to assess the similarities and differences in simvastatin response in another drug sensitive bacterium. We selected *B. thetaiotaomicron* due to its robust genetic tools[18] and to compare a Gram-negative bacterium to the Gram-positive *E. lenta.* As done previously for *E. lenta,* we grew *B. thetaiotaomicron* to mid-exponential phase then added 3 concentrations of simvastatin [low, med, high; 0.1-1X MIC] or vehicle controls at mid-exponential growth. Samples were collected 15 minutes later and used for RNA-seq and analysis.

Remarkably, *B. thetaiotaomicron* exhibited an even more dramatic transcriptional response to simvastatin than *E. lenta.* Principal components analysis revealed clear grouping of the overall transcriptomes of all three doses relative to vehicle controls (**Figure 2.5**); all three doses were statistically significant relative to vehicle controls (R^2=0.47 and p=0.003, PERMANOVA; comparing simvastatin doses to vehicle controls). The number of differentially expressed genes (FDR<0.1 and $|\log_2$ fold-change$|$>1, DESeq2) was higher than *E. lenta* overall but still dose-dependent (**Figure 2.5**), ranging from 115-473 upregulated and 8-468 downregulated genes relative to vehicle controls. At the highest dose, 19% of *B. thetaiotaomicron* genes (879/4,650) were differentially expressed. 31 differentially expressed genes were independent of dose; whereas 619 were consistently altered at the two higher doses (**Figure 2.5**). Pathway enrichment analysis demonstrated a dose-independent enrichment for differentially expressed genes involved in oxidative phosphorylation (**Figure 2.5**). The highest dose also affected genes involved in histidine, glyoxylate/dicarboxylate, and galactose metabolism pathways,

whereas the lowest dose affected genes involved drug (beta-lactam) resistance and the TCA cycle (**Figure 2.5**).

Interestingly, many of the top differentially expressed genes encoded the subunits of 3 distinct multidrug efflux systems (**Figures 2.6**). All of these systems are homologous to the AcrAB-TolC system in *E. coli*, which enables the efflux of a wide variety of compounds, including antibiotics[25]. Similar to *E. coli,* each efflux system in *B. thetaiotaomicron* includes three major subunits, all of which are differentially expressed in response to simvastatin: (*i*) the hydrogen-dependent inner membrane transporter AcrB; (*ii*) the periplasmic membrane fusion protein AcrA; and (*iii*) the outer membrane channel protein TolC[25]. Gene order is conserved in the 3 putative *B. thetaiotaomicron* AcrAB-TolC efflux systems (**Figure 2.6**). Although the *B. thetaiotaomicron* systems remain uncharacterized at the biochemical level, we recently used transposon mutagenesis to implicate one of the 3 systems (encoded by the genes BT3337-9; referred to herein as AcrAB-TolC1) in resistance to the antibiotics fusidic acid and cefoxitin, and the antipsychotic chlorpromazine[18].

In order to test the impact of all three efflux systems on growth in presence of simvastatin, we turned to our previously published barcoded transposon sequencing library[18]. This barcoded transposon mutant library carries transposon insertions in 4,055 non-essential genes whose change in abundance can be measured in the presence of a stressor, previously described as a genome-wide fitness assay[18]. We performed a fitness assay in which we grew up the transposon mutant library in the presence of low [0.1X MIC] levels of simvastatin or vehicle and then looked at the differential abundance of the gene insertions relative to the vehicle. In total, we identified 102 genes that have

significantly improved growth in simvastatin when disrupted and 117 genes whose insertions had significantly impaired growth (FDR<0.1, $|\log_2$ fold-change$|$>1, DESeq2). The genes that exhibited increased growth upon transposon insertion included cardiolipin synthetase (BT3978), potentially suggesting that cardiolipin incorporation into the inner membrane increases simvastatin sensitivity[26]. On the other hand, we noted multiple genes important for simvastatin tolerance, including the transporter system encoded by BT3337-BT3339 (referred to herein as AcrAB-TolC1), important for fusidic acid tolerance[18] (**Figure 2.6**).

We performed a more in-depth analysis of the three *B. thetaiotaomicron* AcrAB-TolC systems that we had previously identified by RNA-seq. The greatest fitness defect was observed when AcrAB-TolC1 was disrupted (**Figures 2.6**), consistent with its high level of baseline gene expression (**Figure S4**). All three systems were significantly induced by low levels of simvastatin, with AcrAB-TolC2 and AcrAB-TolC3 showing the most dramatic upregulation (**Figures 2.6** and **Figure S4**).

Follow-up experiments confirmed that the sensitivity of *B. thetaiotaomicron* to simvastatin was increased in response to chemical and genetic disruption of drug efflux. We used phenylalanine-arginine β-napthylamide (PAβN), which inhibits RND family drug efflux systems, including AcrAB-TolC[27]. The *B. thetaiotaomicron* MIC for simvastatin significantly decreased in response to PAβN (**Figure 2.7**). We obtained stocks with transposon insertions in each of the three *B. thetaiotaomicron tolC* genes[28]. Transposon insertions in two of the loci (*tolC1::Tn* and *tolC3::Tn*) resulted in a lower MIC for simvastatin relative to *wt* (**Figure 2.7**). These results are generalizable to other species; disruption of the single *tolC* encoded by *Escherichia coli* (*ΔtolC::KanR)* led to a significant

increase in simvastatin sensitivity (**Figure 2.7**). Interestingly, while AcrAB-TolC systems are prevalent in members of the Bacteroidota and Proteobacteria, they vary in copy number; Bacteroidota strains can have a maximum of up to 76 systems, while Proteobacteria a maximum of 2 (**Figure S5**)**.** These results, together with another recent report[15], highlight the key role of multi-drug efflux systems in bacterial resistance to both antibiotics and host-targeted drugs.

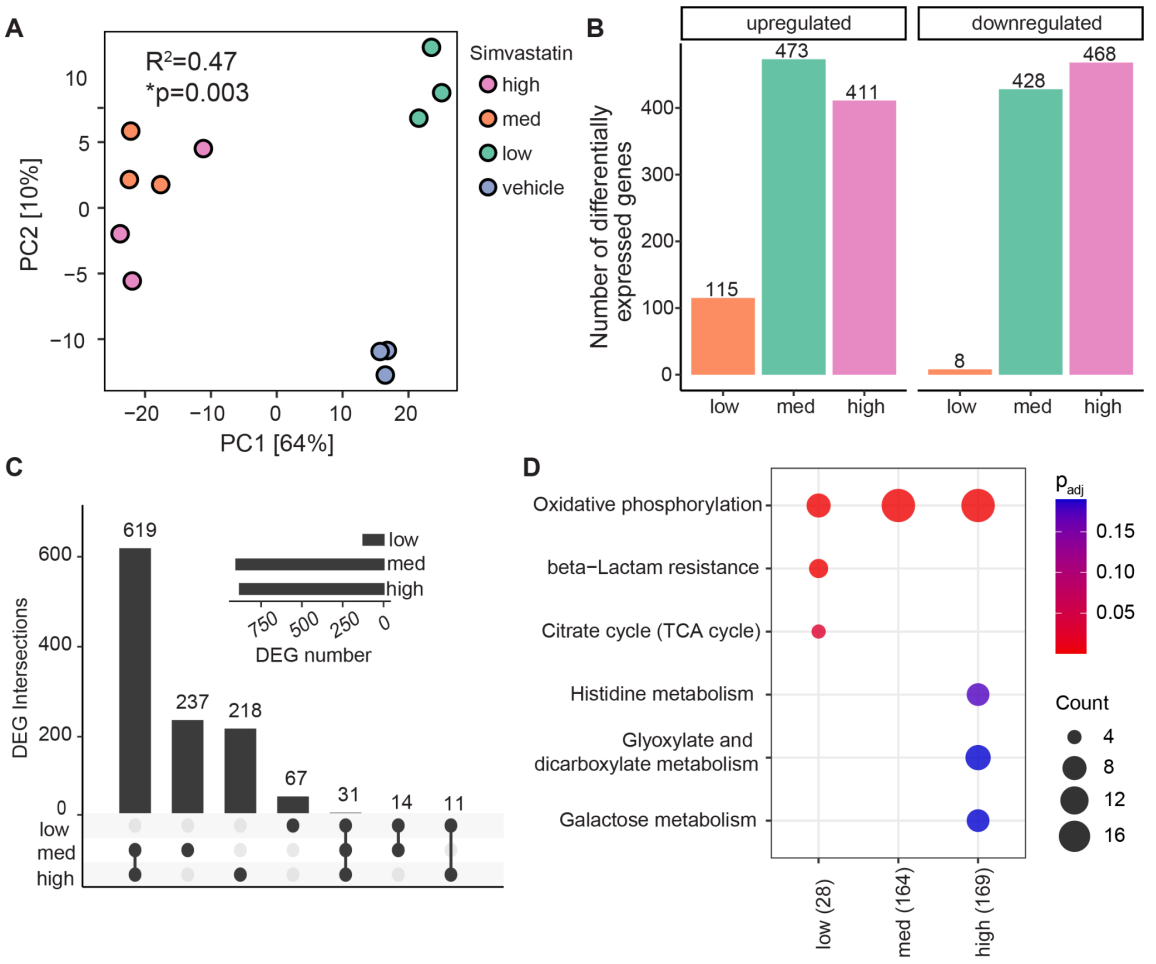

Figure 2.5 Simvastatin has a dose-dependent effect on the *B. thetaiotaomicron* transcriptome. (A) PCA of *B. thetaiotaomicron* DSM2079 RNA-seq data comparing three doses of simvastatin to vehicle controls: low, low-dose (5 μg/mL); med, medium-dose (25 μg/mL); high, high dose (50 μg/mL). Statistical results of PERMANOVA are reported (n=3 biological replicates/group). (B) Number of differentially expressed genes (DEGs; FDR<0.1 and $|\log_2$ fold-change$|$>1 DESeq2) comparing each simvastatin dose relative to vehicle controls. (C) Overlap between DEGs across simvastatin doses. (D) KEGG pathway enrichments for DEGs (p_{adj}<0.2, Benjamini–Hochberg correction): colors, $\log_{10}$ p_{adj}; count, number of DEGs. (B-D) n=2-3 biological replicates/group; one sample from the high-dose simvastatin group was excluded due to low sequencing depth.

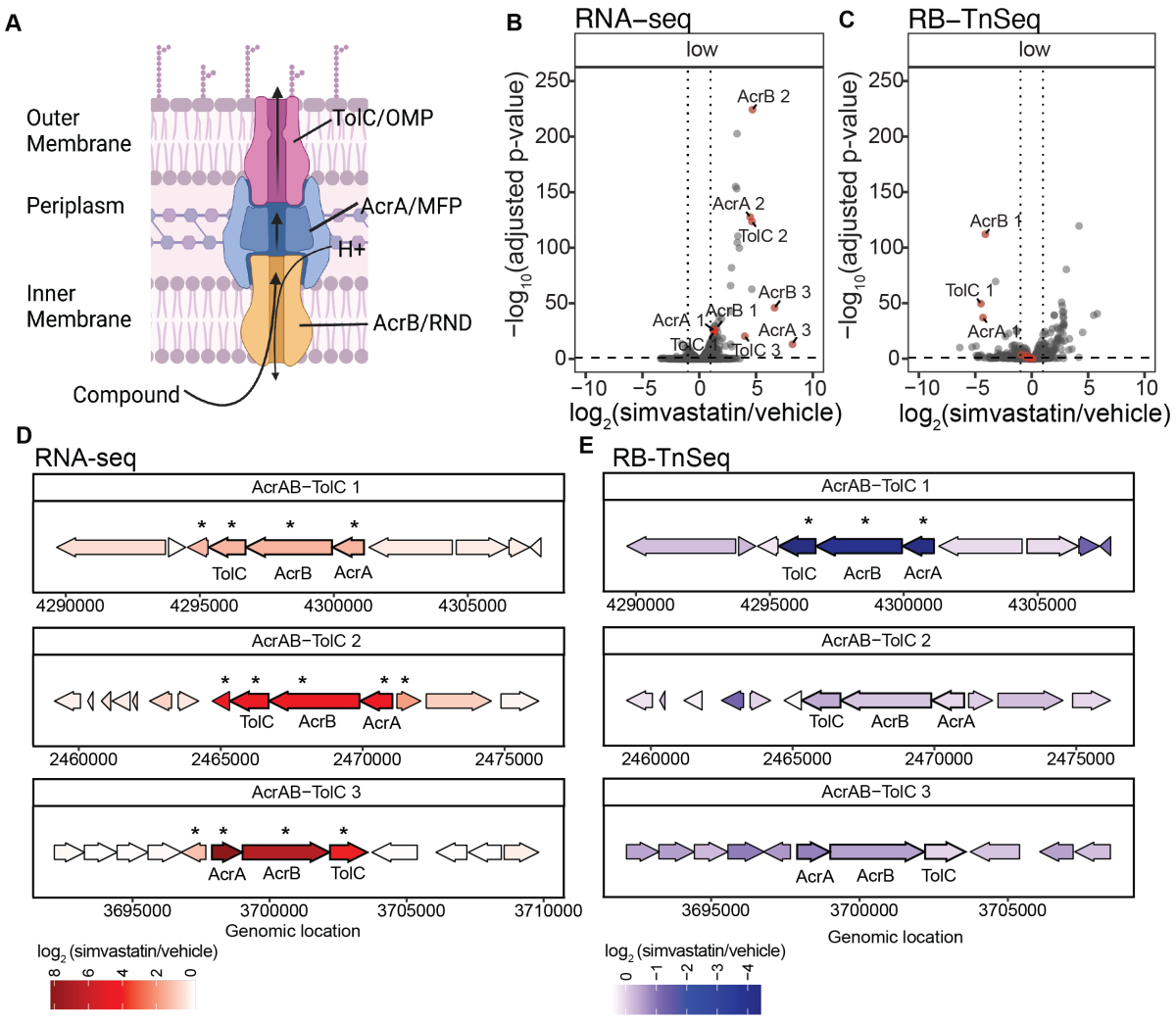

Figure 2.6 Simvastatin induces drug efflux systems in *B. thetaiotaomicron* that enable growth. (A) Schematic of a characterized Resistance-Nodulation-Division (RND) family efflux system [adapted from[29]]. (B-C) Volcano plots of RNA-seq (B) and RB-TnSeq (C) following exposure of *B. thetaiotaomicron* to a low dose of simvastatin relative to vehicle controls (5 µg/mL, 0.1X MIC, n=3 biological replicates/group). Genes homologous to the RND family efflux system BT3337-BT3339/AcrAB-TolC1[18] are labeled red. Points above the horizontal dotted line and to the right and left of the vertical dotted lines have an FDR<0.1 and $|\log_2$ fold-change$|>1$ (DESeq2). (D-E) Genomic loci in *B. thetaiotaomicron* containing RND efflux genes and neighboring genes. Asterisks indicate genes differentially abundant in the presence of simvastatin relative to vehicle controls. (B-E) AcrAB-TolC1 refers to BT3337-BT3339; AcrAB-TolC2 refers to BT1965-1967; AcrAB-TolC3 refers to BT2940-BT2942.

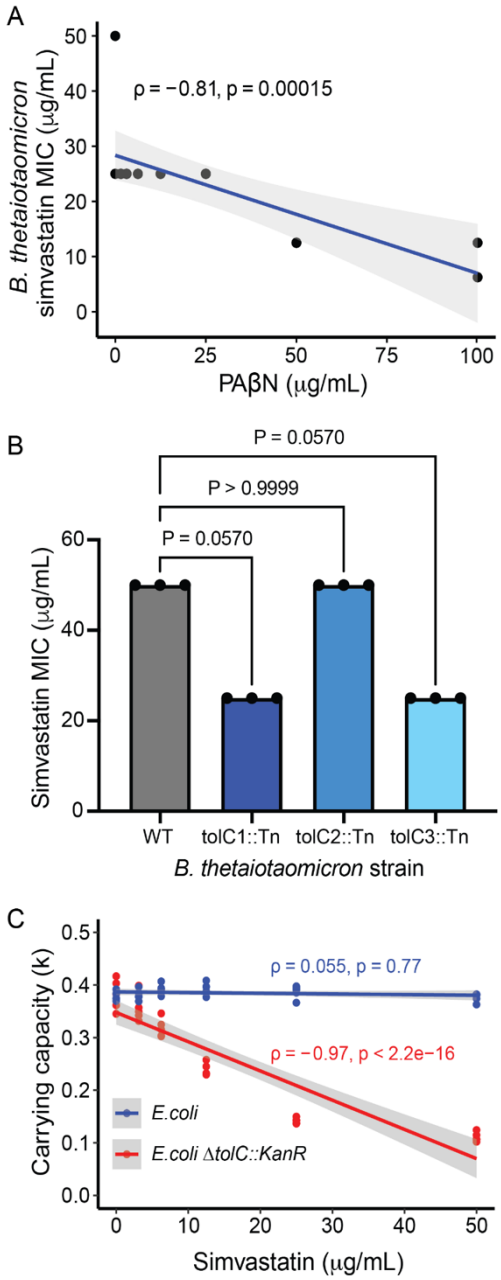

Figure 2.7 RND family drug efflux systems decrease simvastatin sensitivity in *B. thetaiotaomicron* and *E. coli*. (A) *B. thetaiotaomicron* simvastatin MIC is decreased in response to the efflux inhibitor PAβN (Spearman ρ=−0.81, *p*=0.00015; n=2 biological replicates/concentration). Regression line and 95% confidence interval are shown. (B) Transposon insertions in individual tolC genes decreases the MIC of simvastatin for *B. thetaiotaomicron*. (Kruskal-Wallis multiple comparison test; n=3 biological replicates/concentration). (C) TolC protects *E. coli* from simvastatin. The *ΔtolC::KanR* strain exhibits significantly lower carrying capacity in response to increasing concentrations of simvastatin (Spearman ρ=−0.97, *p*<2.2e−16; n=3 biological replicates/concentration). Regression lines and 95% confidence intervals are shown.

2.3 Discussion

Our results demonstrate that simvastatin elicits a direct antibacterial effect on a broader range of human gut bacteria than previously appreciated[15,30]. A prior *in vitro* screen identified a single dose of simvastatin (8.37 μg/mL, 20 μM) that affected the growth of 3 gut bacterial isolates (*P. distasonis*, *R. torques* and *R. intestinalis*) in mono-culture[15]. In this study, we expanded the list of simvastatin-sensitive strains by testing a range of physiologically relevant drug concentrations on human gut bacterial communities and a panel of gut bacterial isolates. Drug sensitivity varied in the context of a community versus pure culture. However, common trends in susceptibility to simvastatin were observed from the phylum- to strain-level. Members of the phylum Bacteroidota were on average more susceptible to simvastatin. A subset of strains from multiple phyla had consistent susceptibility to simvastatin when present in either a community or in isolation, including *B. thetaiotaomicron* and *E. lenta*, which we chose for more in-depth follow-up experiments.

It remains perplexing that simvastatin has direct antimicrobial effects given that HMG-CoA reductase, the canonical target of simvastatin, is rare in human gut bacterial genomes[16,31]. More work is needed to elucidate the mechanism(s) of action that leads to the observed inhibition of diverse gut bacterial species.

Our results indicate that simvastatin has a broad impact on gut bacterial gene expression. These results mirror our prior work on the antimetabolite drugs methotrexate and 5-fluorouracil which demonstrate the marked effect drug exposure can have on gut bacterial transcriptional activity[3,4]. This suggests that simvastatin either directly or

indirectly alters the core metabolic pathways of gut bacteria which are often essential and not reflected in loss-of-function screens. A gain-of-function screen using a barcoded overexpression bacterial shotgun expression library sequencing (Boba-seq), might help complement some of our findings and has the advantage of capturing essential genes[32]. Future studies utilizing affinity probes[33] or other chemical biology tools could help to identify proteins that directly interact with simvastatin within bacterial cells, complementing the bacterial genetic and transcriptomic tools used in this study.

The bacterial cell membrane and its changes in permeability from the incorporation of fatty acids play a key role in antibiotic resistance[34,35]. This has been established for antibiotics like ciprofloxacin[35], but not for antibacterial statins. Here, we found that *E. lenta* responds to simvastatin via the upregulation of genes for fatty acid biosynthesis. More work is needed to explore exactly how the enhanced biosynthesis of fatty acids might contribute to simvastatin resistance. This can be studied by employing fatty acid biosynthesis inhibitors[35] like triclosan and 2-aminooxazole in synergy with simvastatin to test how their combination affects simvastatin susceptibility and cell morphology.

We also found that a subset of transcriptional regulators from the MarR family are upregulated by *E. lenta* in response to simvastatin. MarR-type regulators generally respond to environmental stress responses, including stress triggered by antibiotics, by controlling a small set of genes often located in the same gene cluster[23,24,36,37]. In *E. lenta*, these MarR homologs appear to regulate multiple gene clusters in response to simvastatin, including genes for membrane biogenesis (fatty acid biosynthesis), increased drug efflux (ABC and MATE transporters), and heat shock response (DnaK). More work is needed to further characterize how simvastatin interacts with MarR to affect

these systems. Dissociation of its genetic target is triggered by ligand binding, which could be due to a direct binding to simvastatin or to another compound that is responsive to simvastatin exposure.

Similarly, our data suggests that the gut bacterium *B. thetaiotaomicron* also uses the cell wall to evade the antibacterial effects of simvastatin. We identified three distinct AcrAB-TolC efflux systems, one of which had been previously characterized as important for the tolerance to the antibacterial fusidic acid which is lipophilic and structurally resembles simvastatin[18]. These systems are all homologous to *E. coli*, which only encodes a single AcrAB-TolC efflux system[38]. More work is needed to assess the substrate-specificity and expression level of *B. thetaiotaomicron*'s different AcrAB-TolC efflux systems and their relative impacts on growth in the presence of simvastatin and other drugs. While all three efflux systems were differentially expressed in the presence of simvastatin, only one of these efflux systems significantly impacted competitive growth in our transposon data, suggesting that system is more important for simvastatin tolerance.

This study has multiple key limitations. The bacterial determinants of susceptibility to simvastatin at the cellular and community level remain to be fully elucidated, but likely involve mechanisms of resistance or other microbe-microbe and host-microbe interactions. Furthermore, it will be important to extend our paired transcriptomic and genetic analyses to additional human gut bacterial species; for example, the simvastatin resistant *Bifidobacterium longum* and *Clostridium sporogenes*, which are both genetically tractable. Of note, prior work has indicated that gut bacteria metabolize simvastatin[39,40], which could potentially influence the variation in drug sensitivity we observed. It remains

to be explored whether any of the responses observed in this study could be attributed to simvastatin metabolites. While bacterial drug sensitivity was evaluated *in vitro*, more work is needed to assess the susceptibility of gut bacteria to simvastatin *in vivo*, including in gnotobiotic and conventionally raised mice or other model species.

These findings open the door to exploring how simvastatin's antibacterial properties can contribute to changes in gut microbiome signatures and how they might explain adverse and beneficial effects from statin intake previously observed in metagenomics-based association studies[2,5]. Our current results clearly demonstrate the feasibility and utility of focused studies of individual non-antibiotic drugs, like simvastatin, that can have unintended effects for diverse members of the human gut microbiota. Such knowledge sets the foundation for further mechanistic dissection of these drug-microbiome interactions while informing ongoing work in humans looking at cross-sectional and longitudinal differences in the gut microbiome of patients on these widely used medications.

2.4 Supplementary Figures

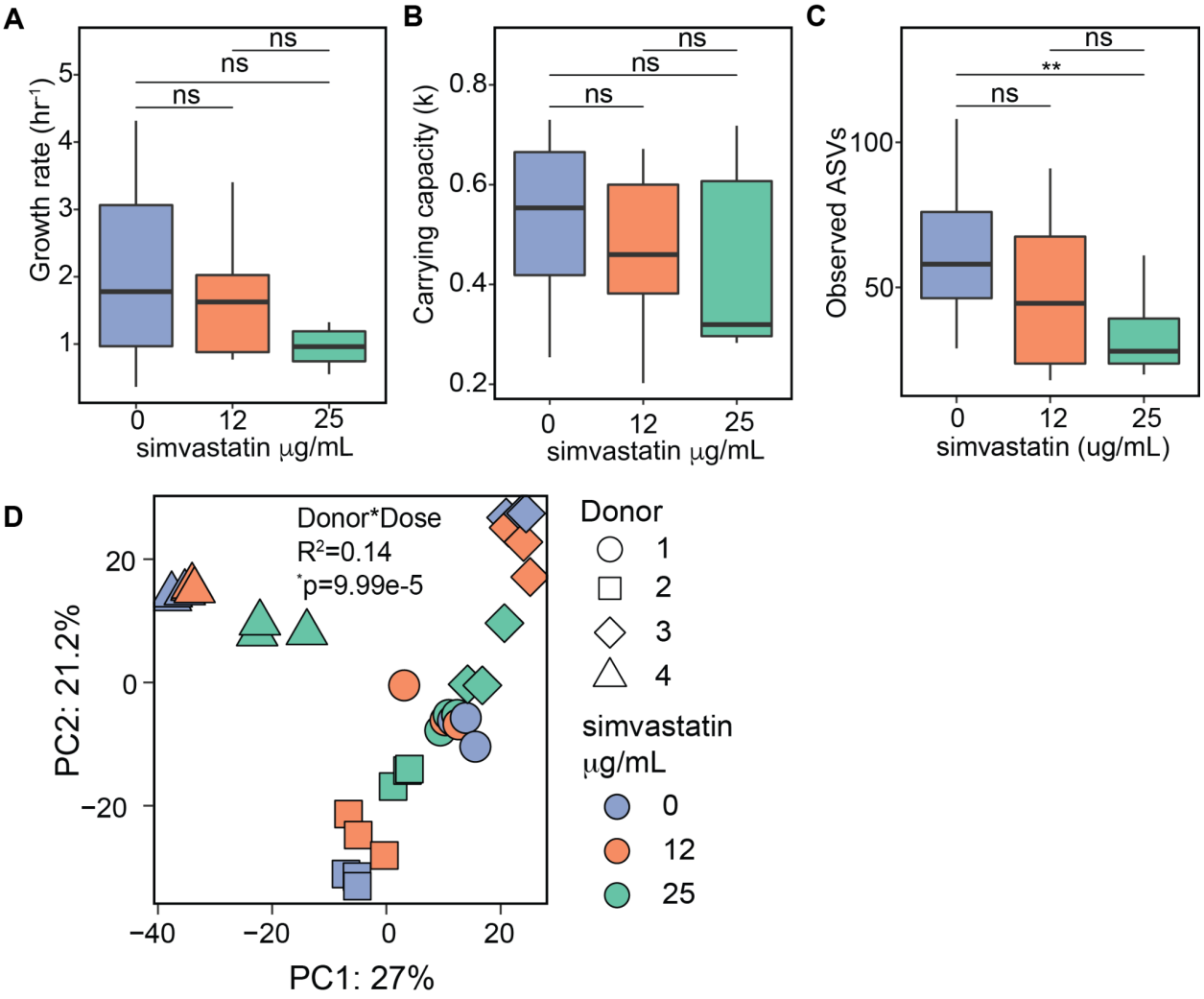

Supplementary Figure S1 Simvastatin alters the human gut microbiota. Human *ex vivo* stool cultures (n=4 donors, n=3 biological replicates/group) were analyzed by 16S rRNA gene sequencing. (A) Growth rate (hr^{-1}). (B) Carrying capacity (k), which denotes the maximum OD_{600} reached by the population (C) Number of ASVs. (D) Principal components 1 and 2 of Euclidean distances using CLR-transformed values from 16S-seq data. Shapes denote different donors and colors denote different simvastatin doses. PERMANOVA revealed a significant interaction of donor with dose.

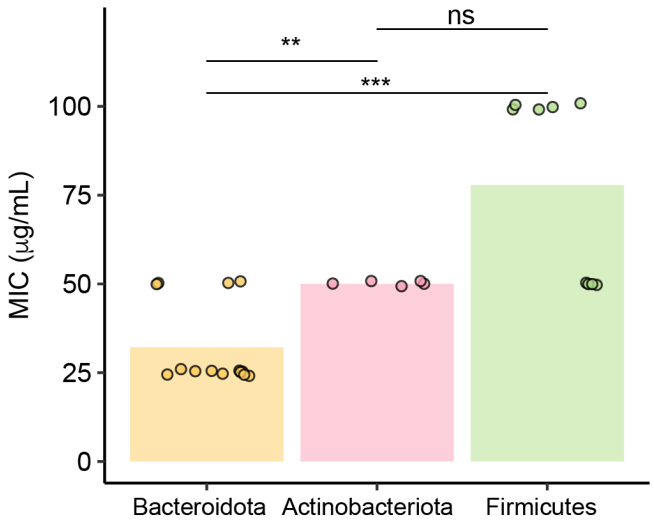

Supplementary Figure S2 Simvastatin sensitivity differs between gut bacterial phyla. MICs (minimum inhibitory concentrations) of isolates from 3 bacterial phyla. Bars represent mean and dots represent each strain. ns, $p>0.05$; **$p<0.01$; ***$p<0.001$, Wilcoxon rank-sum test.

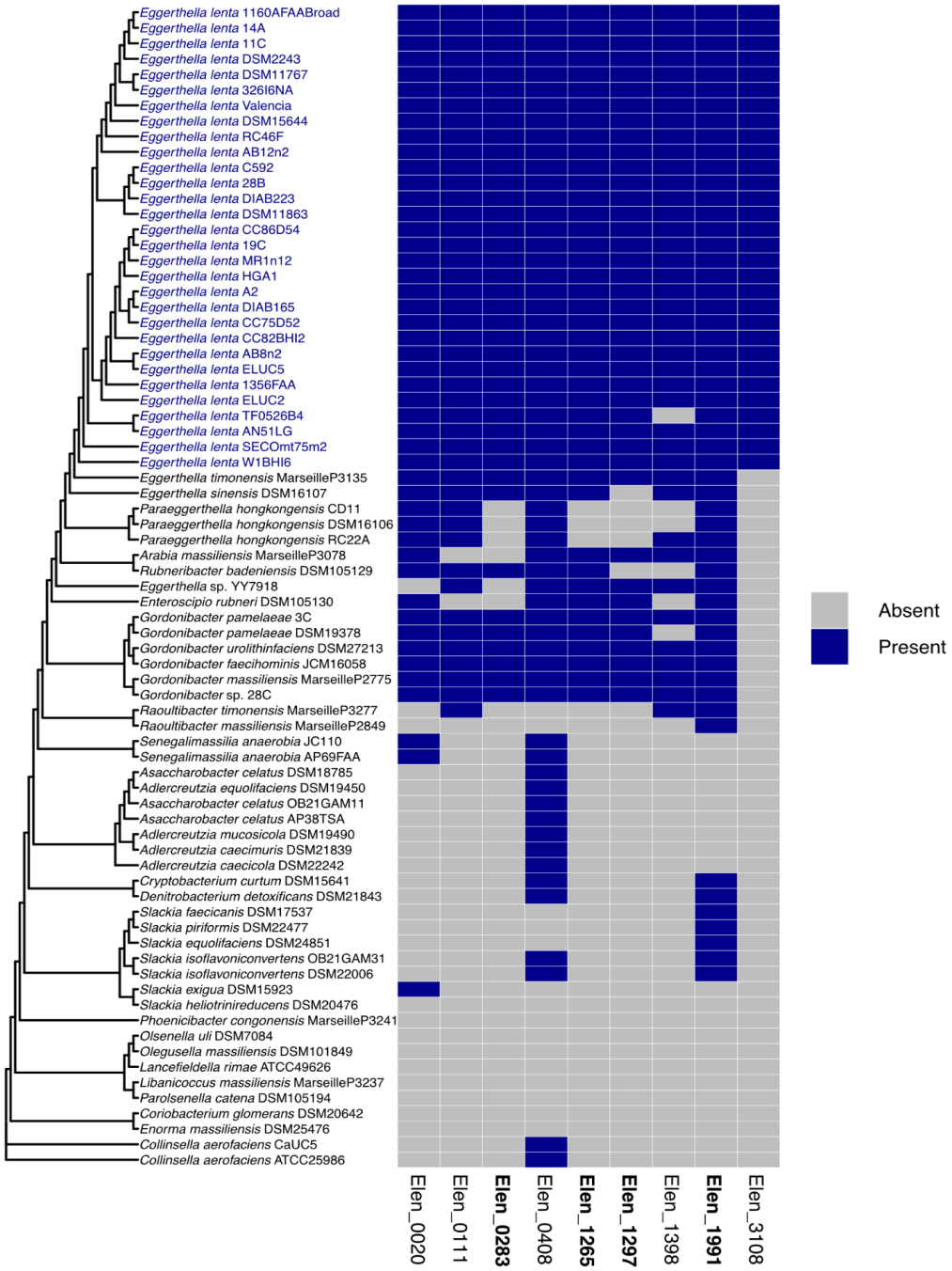

Supplementary Figure S3 Conservation of marR genes across the Coriobacteriia. The heatmap shows the presence or absence of gene families annotated as marR genes in the *E. lenta* DSM2243 genome across gut Coriobacteriia isolate genomes, based on a previous pan-genome analysis[19]. Genes are labeled with their locus tag in the *E. lenta* DSM2243 genome. Gene labels in bold indicate those that were differentially expressed in response to simvastatin treatment. Blue text indicates strains within the *E. lenta* species, in which these genes were near-universally present.

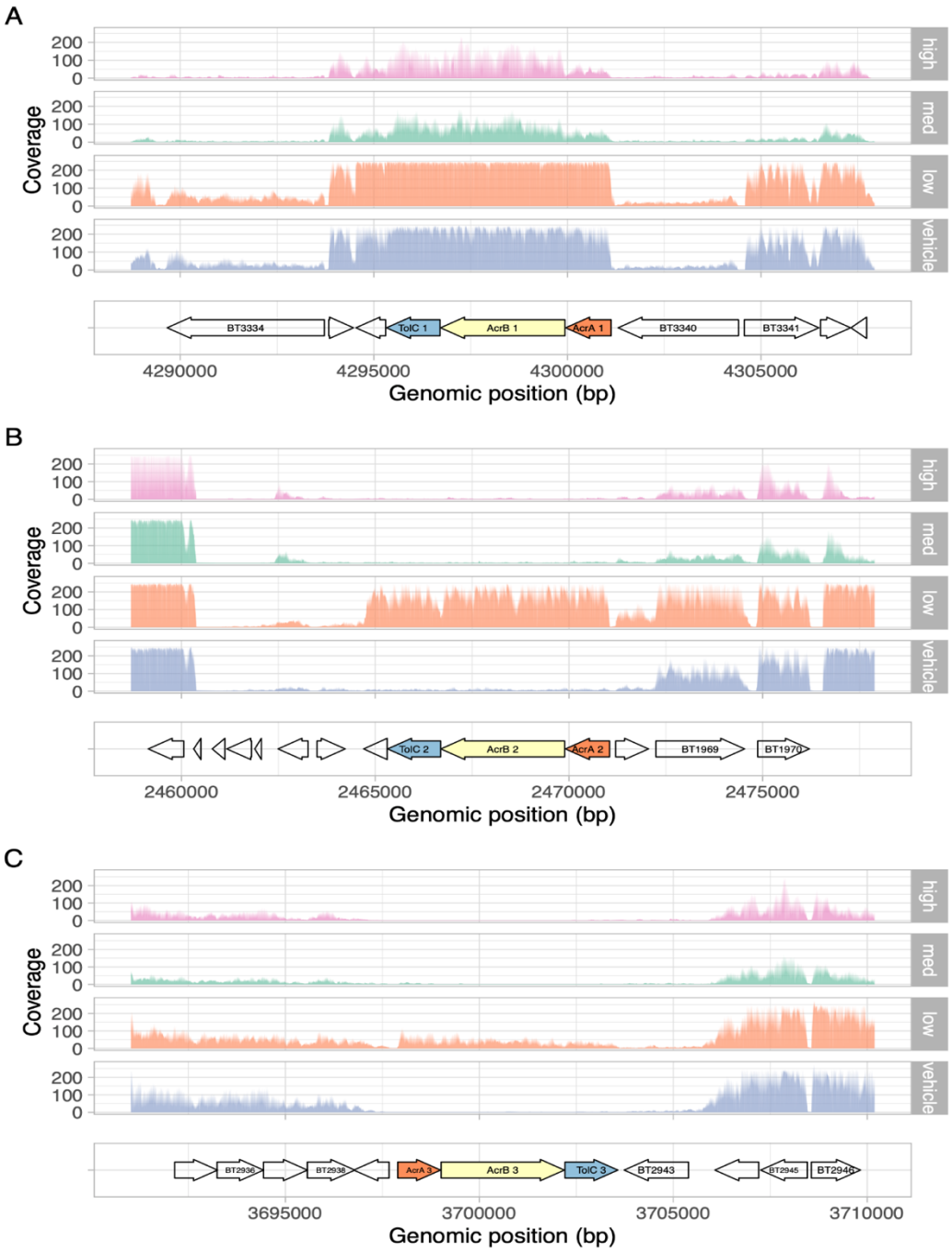

Supplementary Figure S4 RNA-seq coverage of *B. thetaiotaomicron* efflux systems in the presence or absence of simvastatin. (A-C) Base coverage of RNA-seq reads corresponding to the three sets of efflux systems and their neighboring genes is described in **Figure 2.6**. AcrAB-TolC1 refers to BT3337-BT3339; AcrAB-TolC2 refers to BT1965-1967; AcrAB-TolC3 refers to BT2940-BT2942. The levels of AcrAB-TolC 1 (A) are high even in the absence of simvastatin, while AcrAB-TolC 2 and AcrAB-TolC 3 levels are increased with low levels of simvastatin.

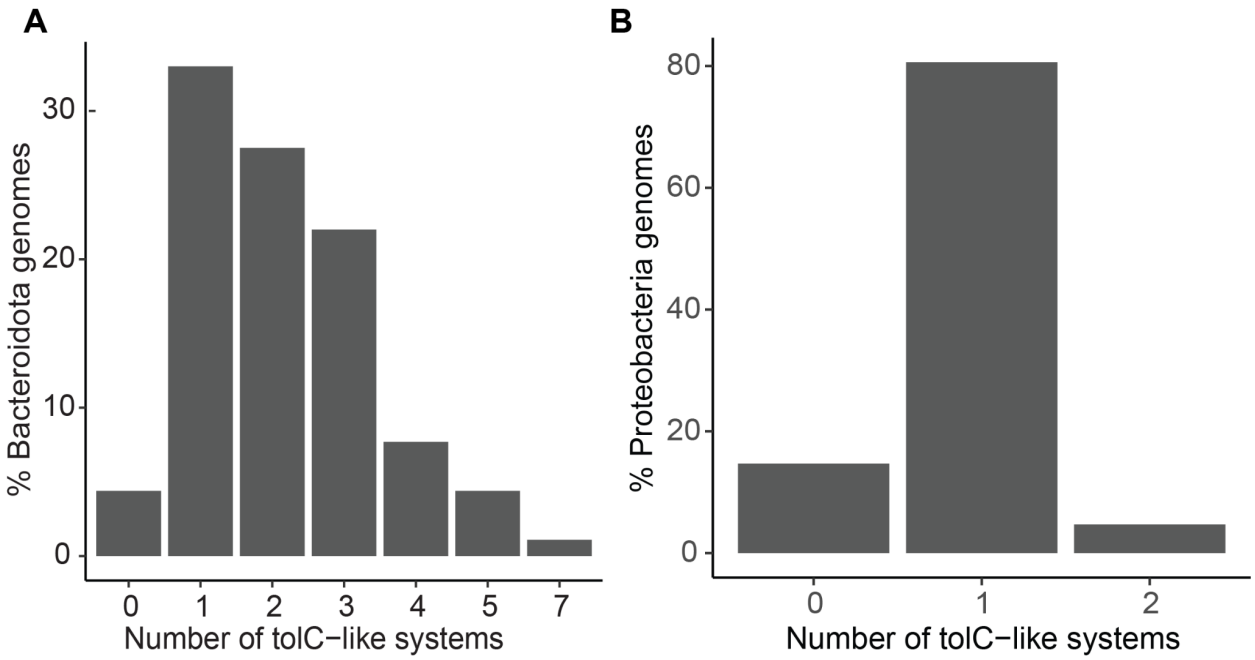

Supplementary Figure S5 TolC-like systems are prevalent across representative human gut bacteria of the Bacteroidota and Proteobacteria phylum. (A-B) Percentage of *tolC*-like systems present in (A) 91 human gut Bacteroidota and (B) 129 human gut Proteobacteria isolate genomes.

2.5 Materials and Methods

Media, strains, and drugs used. BHI^{CHAV}: Bacto Brain Heart Infusion (BD Biosciences, 37 g/L) supplemented with L-cysteine-HCl (0.05%, w/v), hemin (5 µg/mL), L-arginine (1.0%, w/v), vitamin K (1 µg/mL). BHI^{CHV}: Bacto Brain Heart Infusion (BD Biosciences, 37 g/L) supplemented with L-cysteine-HCl (0.05%, w/v), hemin (5 µg/mL), vitamin K (1 µg/mL). Simvastatin: Toronto chemicals S485000. DMSO (anhydrous, ≥99.9%): Sigma-Aldrich Sure/Seal 276855. MeOH (anhydrous, ≥99.9%): Sigma-Aldrich Sure/Seal 294829.

***Ex vivo* incubations of human stool samples.** Stool from four human donors, previously frozen at -80°C upon collection, was aliquoted into a pre-equilibrated cryovial, weighed, diluted in reduced BHI^{CHV} at 10 mL per 1 gram of stool (0.1 g/mL) and vortexed to homogenize. Each sample was allowed to settle for 5 minutes and 100 µL of the sediment-free supernatant aliquoted into a new pre-equilibrated cryovial. Growth was evaluated by inoculating sterile BHI^{CHV} with 1:10 dilution of this fecal slurry, with OD_{600} readings performed every 15 minutes for 48 hours with a 1-min shake prior to each absorbance reading at 37 °C using an Eon Microplate Spectrophotometer (Biotek Instruments, Inc.). Simvastatin dilutions were made from a freshly prepared base stock of 2.5 mg/mL in DMSO. Samples were treated with either simvastatin (25 µg/mL and 12 µg/mL) or an equal volume of 4% DMSO in a final volume of 100 µL prior to placing in the plate reader. Each donor's stool inoculation and treatment were evaluated in triplicate (3 replicates per treatment group). Samples were collected at the experimental endpoint to perform 16S rRNA gene sequencing (16S-seq) and analysis. All work described above was carried out in an anaerobic COY chamber. Growth curves were averaged by

treatment and individual, and growth parameters (time to mid-exponential, carrying capacity and growth rate) were estimated using the Growthcurver package[41]. ANOVA was used to determine changes in growth parameters between groups. The maximal intestinal concentration of simvastatin was calculated as previously described[42]: 40 mg recommended daily dose (source:simvastatin package insert) divided by 250 mL. Distal gut levels were estimated based on isotope labeling experiments indicating that 60% of the administered dose is excreted in stool[43] (DrugBank accession: DB00641).

16S-seq and analysis of *ex vivo* incubations with simvastatin. Bacterial pellets from the *ex vivo* incubations above (100 µL) were collected by centrifugation at 3,000 rpm for 5 min and then stored at -80 °C. DNA was extracted using a ZymoBIOMICS 96 MagBead DNA Kit (Zymo D4308) as per the manufacturer's protocol, and 16S rRNA amplicon library was constructed following a dual-indexing approach[44]. Samples underwent 16S rRNA gene amplification using GoLay-barcoded V4 region V4-515F and V4-806R primers[44] on a BioRad CFX 384 real-time PCR instrument with four serial 10 fold dilutions of extracted DNA template. Individual sample dilutions in the exponential phase were manually selected for subsequent indexing PCR using a dual GoLay index primers to add flow cell adaptors and indices as previously described[44]. DNA concentration was measured using a PicoGreen assay (P7589, Life Technologies) and samples were pooled at equimolar concentrations. Pooled libraries were purified and concentrated with MinElute PCR Purification kit (Qiagen #28004), run on 1% gel, size-selected (~427 bp) and purified using MinElute Gel Extraction kits (Qiagen, #28604). Libraries were quantified (NEBNext Library Quantification Kit; New England Biolabs) and sequenced with a 600 cycle MiSeq Reagent Kit v3 (paired-end reads set up for 250X8X8X250;

Illumina MiSeq) with 15% PhiX spiked in before sequencing at the UCSF Center for Advanced Technology.

QIIME2[45] was used to trim primer reads, denoise the data and create a feature table using the following: *qiime cutadapt trim-paired*, *qiime dada2 denoise-paired*, and *qiime feature-classifier classify-sklearn* as in our lab pipeline (https://github.com/jbisanz/16Spipelines/blob/master/QIIME2_pipeline.Rmd). Taxonomy was assigned using DADA2[46] with implementation of the RDP classifier[47] using the DADA2-formatted SILVA v128 training set. A phylogenetic tree was constructed using QIIME2 and the command *phylogeny align-to-tree-mafft-fasttree*. QIIME2 artifacts were imported into R using the qiime2R package (https://github.com/jbisanz/qiime2R). Low abundance taxa present in less than 3 samples and with less than 10 reads were filtered out. We assigned a unique ASV identifier that can be used to look up a full taxonomic assignment, from kingdom to species, associated with a sequence variant. Diversity metrics were generated using vegan[48] and phyloseq[49] packages in R. Principal coordinates analysis (PCoA) or Principal components analysis (PCA) were performed with ape[50] or vegan packages, respectively. Analyses were carried out using the centered $\log_2$-ratio (CLR) normalized taxonomic abudances A_{clr} = [$\log_2(A_1/g_a)$, $\log_2(A_2/g_a)$,… $\log_2(A_n/g_a)$], where A is a vector of read counts with a prior of 0.5 added and g_a is the geometric mean of all values of A. Taxa were merged at different taxonomic levels using *tax_glom* from the phyloseq package before being CLR transformed where applicable. PERMANOVA was employed to detect changes in community composition from rarified counts or Bray-Curtis distances. Differential abundant ASVs were determined by employing ALDEx2[51,52] using 150 simulations.

***In vitro* bacterial growth studies**. Each of these strains was obtained from the Deutsche Sammlung von Mikroorganismen und Zellkulturen (DSMZ) culture collection. A single colony of each isolate was sub-cultured in 5 mL of BHI^{CHAV} for 48 hours in an anaerobic chamber (Coy Laboratory Products) at 37°C with an atmosphere composed of 2-3% H_2, 20% CO_2, and the balance N_2. This subculture was diluted down to an OD_{600} of 0.1, which was then further diluted 100-fold, and then used to inoculate a microtiter plate with 2-fold serial dilutions of simvastatin concentrations ranging from 1.5625 – 100 μg/mL or a 4% DMSO/MeOH vehicle control in a final volume of 100 μL. DMSO was used as a vehicle control for most of the isolates, except for the isolates from the Actinobacteria phylum which we found did not tolerate DMSO well and MeOH was used instead. Higher concentrations of simvastatin were not tested due to solubility limits in BHI^{CHAV}. Plates were incubated at 37°C over a 48-hour period in the anaerobic chamber and growth assessed by a final OD_{600} measurement. The minimal inhibitory concentration (MIC) was measured as the lowest concentration of simvastatin resulting in >90% growth inhibition after 48 hours of incubation. Absorbance of cultures in 96-well plates were read using an Eon Microplate Spectrophotometer (BioTek Instruments, Inc).

Tree construction. Full-length ribosomal sequences for each isolate were extracted from the database greengenes[53]. Sequences were imported into Unipro UGENE[54] and aligned using MUSCLE[55]. Gaps occurring in >50% of sequences were removed and a maximum likelihood tree generated using PhyML[56]. For trees generated from 16S-seq from *ex vivo* samples, we used the ggtree R package[57].

Bacterial incubations for transcriptional profiling. Bacterial isolates *E. lenta* DSM 2243 and *B. thetaiotaomicron* DSM 2079 were grown anaerobically in previously

equilibrated BHI^{CHAV} at 37 °C. Cultures for each isolate were grown to mid-exponential phase, split into triplicates, and incubated for 15 min at a range of simvastatin concentrations (1X, 0.5X, and 0.1X MIC) or vehicle. Following incubations, cultures were removed from the anaerobic chamber in sealed Falcon tubes and placed immediately on ice. Cultures were centrifuged at 3,000 rpm for 5 min at 4 °C, the supernatant removed, and the bacterial pellets flash-frozen in liquid nitrogen for future RNA extraction.

RNA extractions. Each bacterial pellet was incubated with 1 mL of Tri Reagent (Sigma Aldrich T9424) at room temperature for 10 minutes. The cell suspension was transferred into Lysing Matrix E tubes (MP Biomedicals, 116914050) and homogenized in a bead-beater (Mini-Beadbeater-24, BioSpec) for 5 minutes at room temperature. The sample was incubated with 200 µL of chloroform at room temperature for 10 minutes, followed by centrifugation at 16,000 g for 15 minutes at 4 °C. Next, 500 µL of the upper aqueous phase was transferred into a new tube and 500 µL of 100% ethanol was added. To isolate RNA, we used the PureLink RNA Mini Kit (Life Technologies, catalog #: 12183025). This mixture was transferred onto a PureLink spin column and spun at ≥ 12,000 × g for 30 seconds. The column was washed with 350 µL of wash buffer I as described in the PureLink manual. The column was incubated with 80 µL of PureLink DNase (Life Technologies, catalog #: 12185010) at room temperature for 15 minutes, and washed with 350 µL of wash buffer I. The column was washed with wash buffer II twice as described in the PureLink manual. Total RNA was recovered in 50 µL of RNAase-free water. A second round of DNAse treatment was undertaken. The RNA was incubated with 6 µL of TURBO DNAse (Ambion, ThermoFisher, catalog #: AM2238) at 37 °C for 30 minutes. To stop the reaction, 56 µL of lysis buffer from the PureLink kit and 56 µL of

100% ethanol was added to the sample and vortexed. This suspension was transferred onto a PureLink column, and washed once with 350 µL of wash buffer I and twice with 500 µL of wash buffer II. The RNA was recovered in 30 µL of RNAse-free water.

rRNA depletion, library generation, and RNA sequencing. Total RNA was subjected to rRNA depletion using the RiboMinus Bacteria Transcription Isolation kit (ThermoFisher, catalog # A47335), following the manufacturer's protocol. RNA fragmentation, cDNA synthesis, and library preparation proceeded using NEBNext Ultra RNA Library Prep Kit for Illumina (New England BioLabs, catalog # E7530) and NEBNext Multiplex Oligos for Illumina, Dual Index Primers (New England BioLabs, catalog # E7600), following the manufacturer's protocol. All samples were paired end sequenced (2x150 bp) using an Illumina NovaSeq platform (NovaSeq 6000 v1.5) at UCSF's Institute for Human Genomics.

RNA sequencing analysis. Reads were trimmed using fastp[58]. Reference genomes were obtained from NCBI's genome assembly database under the following accession numbers: ASM2426v1 for *E. lenta* and ASM1106v1 for *B. thetaiotaomicron*. Reads were mapped to reference genomes using Bowtie2[59] using the following options: *q, --met-file, --end-to-end, --sensitive.* HTSeq[60] was used to count the number of transcripts mapping to genes using the following options: *--type*=CDS, *--idattr:*ID, *--stranded*=no, *--minaqual*=10*.* Differential abundance of gene transcripts in the simvastatin treated (low, med, high) and untreated samples was assessed using DESeq2[61] (v1.26.0) with the *DeSeqDataSetFromHTSeqCount* and *ddsHTSeq* functions and their default options. Different FDR thresholds ranging from 0.01 to 0.1 were used to determine the number of differentially expressed genes, and irrespective of the threshold used, consistent

percentages of each bacterial genome were affected by simvastatin. Ultimately, a threshold of FDR<0.1 and |$\log_2$ fold-change|>1 was chosen to determine significance. BlastKOALA[62] was used to map protein sequences from each organism to KO terms using the "species_prokaryote" database. KEGG pathway enrichment was carried out using clusterProfiler[63] (v3.14.3) and the enrichKEGG function. KO terms for all differentially abundant barcodes (both up- and down- regulated with a p_{adj}<0.1, DESeq2 and |$\log_2$ fold-change|>1) were provided and the organism parameter was set to "ko". Heatmaps and volcano plots were generated using the ggplot2 R package[64] (v3.3.5).

***In vitro* transposon mutant fitness assays and barcode sequencing.** We performed *B. thetaiotaomicron* transposon mutant fitness assays as described previously[18]. For *B. thetaiotaomicron*, we thawed an aliquot of the full transposon mutant library, inoculated the entire aliquot into 50 mL of BHIS supplemented with 10 µg/mL erythromycin, and grew the library to mid-log phase. We then collected 6 cell pellets of ~1.0 OD_{600} unit each (the "Time0" sample). We used the remaining cells to inoculate competitive growth assays in the presence of simvastatin or a vehicle control. All fitness assays were performed in 1.2 mL of growth medium in a 24-well transparent microplate (Greiner) at a starting OD_{600} of 0.02. We grew cultures until the vehicle group reached stationary phase, and then collected cell pellets (the "Condition" sample). We extracted genomic DNA from the Time0 and Condition samples in a 96-well microplate format with a ZymoBIOMICS 96 MagBead DNA kit (ZymoResearch, catalog # D4302). We performed barcode sequencing (BarSeq) as previously described[18,65]. We used BarSeq oligos with both P1 and P2 indexed to minimize the impact of incorrectly assigned indexes in Illumina HiSeq4000 runs [66]. Strain and gene fitness scores were calculated as previously described and can be found within

the Fitness Browser (https://fit.genomics.lbl.gov)[67]. Fitness values are $\log_2$ ratios that describe the change in abundance of mutants in that gene during the experiment. For most of the fitness experiments, which are growth experiments, the change reflects how well the mutants grow relative to the "Time0" samples. The "Time0" samples also serve as a control to ensure the number of mutants across an experiment are consistent with previous fitness assays.

Transposon sequencing analysis. Barcoded transposon insertions were summed for each gene. Differential abundance of the individual genes in the treated and untreated mutant populations was assessed using DESeq2[61] (v1.26.0) with the *DeSeqDataSetFromMatrix* and *dds* functions and their default options on the gene count matrix. A threshold of FDR<0.1 and $|\log_2$ fold-change$|>1$ was used to determine significance. BlastKOALA [62] was used to map protein sequences from each organism to KO terms using the "species_prokaryote" database. KEGG pathway enrichment was carried out using clusterProfiler[63] (v3.14.3) using the enrichKEGG function. KO terms for all differentially abundant barcodes (both up- and down- regulated with a FDR<0.1, DESeq2 and $|\log_2$ fold-change$| > 1$) were provided and the organism parameter was set to "ko". Heatmaps and volcano plots were generated using the ggplot2 R package [64] (v3.3.5).

Comparative genomics. A previous pan-genome analysis[19] was used to assess conservation of marR genes across gut Coriobacteriia isolate genomes defined using ProteinOrtho v6.0.6[68], with gene family cutoffs of 60% identity and 80% coverage. marR gene families were defined based on annotation of the *E. lenta* DSM 2243 genome using InterProScan[69]. Our results were largely unchanged when using a looser sequence

identity cutoff (40%). The United Human Gastrointestinal Genome collection (v2.0.1) was used to assess conservation of tolC-like systems across human gut microbes. The 4,744 species representative genomes and corresponding eggNOG-db annotations (https://doi.org/10.1093/nar/gky1085) were downloaded from the MGnify database, including 619 assigned to the Bacteroidota phylum (91 isolates and 528 metagenome-assembled genomes) (https://doi.org/10.1016/j.jmb.2023.168016). The following phylum-level eggNOG gene families were used to define the *B. thetaiotaomicron*-like tolC gene cluster: 4NEXN (BT_3339), 4NDZG (BT_3338) and 4NDZK (BT_3337). All 3 gene families were required to be adjacent to each other to be counted as a complete system, as in the *B. thetaiotaomicron* genome. The following phylum-level eggNOG gene families were used to define the *E. coli*-like tolC genes in Proteobacteria: 1MU78 (b0463), 1MU48 (b0462), and 1MWCJ (b3035). These were not required to be adjacent.

2.6 References

1. Falony, G., Joossens, M., Vieira-Silva, S., Wang, J., Darzi, Y., Faust, K., Kurilshikov, A., Bonder, M.J., Valles-Colomer, M., Vandeputte, D., et al. (2016). Population-level analysis of gut microbiome variation. Science *352*, 560–564.

2. Zhernakova, A., Kurilshikov, A., Bonder, M.J., Tigchelaar, E.F., Schirmer, M., Vatanen, T., Mujagic, Z., Vila, A.V., Falony, G., Vieira-Silva, S., et al. (2016). Population-based metagenomics analysis reveals markers for gut microbiome composition and diversity. Science *352*, 565–569.

3. Spanogiannopoulos, P., Kyaw, T.S., Guthrie, B.G.H., Bradley, P.H., Lee, J.V., Melamed, J., Malig, Y.N.A., Lam, K.N., Gempis, D., Sandy, M., et al. (2022). Host and gut bacteria share metabolic pathways for anti-cancer drug metabolism. Nature Microbiology *7*, 1605–1620. 10.1038/s41564-022-01226-5.

4. Nayak, R.R., Alexander, M., Deshpande, I., Stapleton-Gray, K., Rimal, B., Patterson, A.D., Ubeda, C., Scher, J.U., and Turnbaugh, P.J. (2021). Methotrexate impacts conserved pathways in diverse human gut bacteria leading to decreased host immune activation. Cell Host Microbe. 10.1016/j.chom.2020.12.008.

5. Vieira-Silva, S., Falony, G., Belda, E., Nielsen, T., Aron-Wisnewsky, J., Chakaroun, R., Forslund, S.K., Assmann, K., Valles-Colomer, M., Nguyen, T.T.D., et al. (2020). Statin therapy is associated with lower prevalence of gut microbiota dysbiosis. Nature *581*, 310–315.

6. Golomb, B.A., and Evans, M.A. (2008). Statin adverse effects : a review of the literature and evidence for a mitochondrial mechanism. Am. J. Cardiovasc. Drugs *8*, 373–418.

7. Kaddurah-Daouk, R., Baillie, R.A., Zhu, H., Zeng, Z.-B., Wiest, M.M., Nguyen, U.T., Wojnoonski, K., Watkins, S.M., Trupp, M., and Krauss, R.M. (2011). Enteric microbiome metabolites correlate with response to simvastatin treatment. PLoS One *6*, e25482.

8. Wilmanski, T., Kornilov, S.A., Diener, C., Conomos, M.P., Lovejoy, J.C., Sebastiani, P., Orwoll, E.S., Hood, L., Price, N.D., Rappaport, N., et al. (2022). Heterogeneity in statin responses explained by variation in the human gut microbiome. Med (N Y) *3*, 388–405.e6.

9. Cheng, T., Li, C., Shen, L., Wang, S., Li, X., Fu, C., Li, T., Liu, B., Gu, Y., Wang, W., et al. (2021). The Intestinal Effect of Atorvastatin: Akkermansia muciniphila and Barrier Function. Front. Microbiol. *12*, 797062.

10. Xu, M., Luo, L.-L., Du, M.-Y., Tang, L., Zhou, J., Hu, Y., and Mei, H. (2022). Simvastatin Improves Outcomes of Endotoxin-induced Coagulopathy by Regulating Intestinal Microenvironment. Curr Med Sci *42*, 26–38.

11. Zhang, P., Zhang, X., Huang, Y., Chen, J., Shang, W., Shi, G., Zhang, L., Zhang, C., and Chen, R. (2021). Atorvastatin alleviates microglia-mediated neuroinflammation via modulating the microbial composition and the intestinal barrier function in ischemic stroke mice. Free Radic. Biol. Med. *162*, 104–117.

12. Caparrós-Martín, J.A., Lareu, R.R., Ramsay, J.P., Peplies, J., Reen, F.J., Headlam, H.A., Ward, N.C., Croft, K.D., Newsholme, P., Hughes, J.D., et al. (2017). Statin therapy causes gut dysbiosis in mice through a PXR-dependent mechanism. Microbiome *5*, 95.

13. Catry, E., Pachikian, B.D., Salazar, N., Neyrinck, A.M., Cani, P.D., and Delzenne, N.M. (2015). Ezetimibe and simvastatin modulate gut microbiota and expression of genes related to cholesterol metabolism. Life Sci. *132*, 77–84.

14. He, X., Zheng, N., He, J., Liu, C., Feng, J., Jia, W., and Li, H. (2017). Gut Microbiota Modulation Attenuated the Hypolipidemic Effect of Simvastatin in High-Fat/Cholesterol-Diet Fed Mice. J. Proteome Res. *16*, 1900–1910.

15. Maier, L., Pruteanu, M., Kuhn, M., Zeller, G., Telzerow, A., Anderson, E.E., Brochado, A.R., Fernandez, K.C., Dose, H., Mori, H., et al. (2018). Extensive impact of non-antibiotic drugs on human gut bacteria. Nature *555*, 623–628.

16. Gill, S.R., Pop, M., Deboy, R.T., Eckburg, P.B., Turnbaugh, P.J., Samuel, B.S., Gordon, J.I., Relman, D.A., Fraser-Liggett, C.M., and Nelson, K.E. (2006). Metagenomic analysis of the human distal gut microbiome. Science *312*, 1355–1359.

17. Maurice, C.F., Haiser, H.J., and Turnbaugh, P.J. (2013). Xenobiotics shape the physiology and gene expression of the active human gut microbiome. Cell *152*, 39–50.

18. Liu, H., Shiver, A.L., Price, M.N., Carlson, H.K., Trotter, V.V., Chen, Y., Escalante, V., Ray, J., Hern, K.E., Petzold, C.J., et al. (2021). Functional genetics of human gut

commensal Bacteroides thetaiotaomicron reveals metabolic requirements for growth across environments. Cell Rep. *34*, 108789.

19. Bisanz, J.E., Soto-Perez, P., Noecker, C., Aksenov, A.A., Lam, K.N., Kenney, G.E., Bess, E.N., Haiser, H.J., Kyaw, T.S., Yu, F.B., et al. (2020). A Genomic Toolkit for the Mechanistic Dissection of Intractable Human Gut Bacteria. Cell Host Microbe *27*, 1001–1013.e9.

20. Sulavik, M.C., Gambino, L.F., and Miller, P.F. (1995). The MarR repressor of the multiple antibiotic resistance (mar) operon in Escherichia coli: prototypic member of a family of bacterial regulatory proteins involved in sensing phenolic compounds. Mol. Med. *1*, 436–446.

21. Perera, I.C., and Grove, A. (2010). Molecular mechanisms of ligand-mediated attenuation of DNA binding by MarR family transcriptional regulators. J. Mol. Cell Biol. *2*, 243–254.

22. Grove, A. (2013). MarR family transcription factors. Curr. Biol. *23*, R142–R143.

23. Lomovskaya, O., Lewis, K., and Matin, A. (1995). EmrR is a negative regulator of the Escherichia coli multidrug resistance pump EmrAB. J. Bacteriol. *177*, 2328–2334.

24. Xiong, A., Gottman, A., Park, C., Baetens, M., Pandza, S., and Matin, A. (2000). The EmrR protein represses the Escherichia coli emrRAB multidrug resistance operon by directly binding to its promoter region. Antimicrob. Agents Chemother. *44*, 2905–2907.

25. Li, X.-Z., and Nikaido, H. (2009). Efflux-mediated drug resistance in bacteria: an update. Drugs *69*, 1555–1623.

26. Davlieva, M., Zhang, W., Arias, C.A., and Shamoo, Y. (2013). Biochemical characterization of cardiolipin synthase mutations associated with daptomycin resistance in enterococci. Antimicrob. Agents Chemother. *57*, 289–296.

27. Lamers, R.P., Cavallari, J.F., and Burrows, L.L. (2013). The efflux inhibitor phenylalanine-arginine beta-naphthylamide (PAβN) permeabilizes the outer membrane of gram-negative bacteria. PLoS One *8*, e60666.

28. Arjes, H.A., Sun, J., Liu, H., Nguyen, T.H., Culver, R.N., Celis, A.I., Walton, S.J., Vasquez, K.S., Yu, F.B., Xue, K.S., et al. (2022). Construction and characterization of a genome-scale ordered mutant collection of Bacteroides thetaiotaomicron. BMC Biol. *20*, 285.

29. Anes, J., McCusker, M.P., Fanning, S., and Martins, M. (2015). The ins and outs of RND efflux pumps in Escherichia coli. Frontiers in Microbiology *6*. 10.3389/fmicb.2015.00587.

30. Ko, H.H.T., Lareu, R.R., Dix, B.R., and Hughes, J.D. (2017). Statins: antimicrobial resistance breakers or makers? PeerJ *5*, e3952.

31. Heuston, S., Begley, M., Gahan, C.G.M., and Hill, C. (2012). Isoprenoid biosynthesis in bacterial pathogens. Microbiology *158*, 1389–1401.

32. Huang, Y.Y., Price, M.N., Hung, A., Gal-Oz, O., Ho, D., Carion, H., Deutschbauer,

A.M., and Arkin, A.P. (2022). Functional screens of barcoded expression libraries uncover new gene functions in carbon utilization among gut Bacteroidales. bioRxiv, 2022.10.10.511384. 10.1101/2022.10.10.511384.

33. Brandvold, K.R., Miller, C.J., Volk, R.F., Killinger, B.J., Whidbey, C., and Wright, A.T. (2021). Activity-based protein profiling of bile salt hydrolysis in the human gut microbiome with beta-lactam or acrylamide-based probes. Chembiochem *22*, 1448–1455.

34. Royce, L.A., Liu, P., Stebbins, M.J., Hanson, B.C., and Jarboe, L.R. (2013). The damaging effects of short chain fatty acids on Escherichia coli membranes. Appl. Microbiol. Biotechnol. *97*, 8317–8327.

35. Su, Y.-B., Kuang, S.-F., Ye, J.-Z., Tao, J.-J., Li, H., Peng, X.-X., and Peng, B. (2021). Enhanced Biosynthesis of Fatty Acids Is Associated with the Acquisition of Ciprofloxacin Resistance in Edwardsiella tarda. mSystems *6*, e0069421.

36. Poole, K., Tetro, K., Zhao, Q., Neshat, S., Heinrichs, D.E., and Bianco, N. (1996). Expression of the multidrug resistance operon mexA-mexB-oprM in Pseudomonas aeruginosa: mexR encodes a regulator of operon expression. Antimicrob. Agents Chemother. *40*, 2021–2028.

37. Srikumar, R., Paul, C.J., and Poole, K. (2000). Influence of mutations in the mexR repressor gene on expression of the MexA-MexB-oprM multidrug efflux system of Pseudomonas aeruginosa. J. Bacteriol. *182*, 1410–1414.

38. Nikaido, H., and Takatsuka, Y. (2009). Mechanisms of RND multidrug efflux pumps.

Biochim. Biophys. Acta *1794*, 769–781.

39. Aura, A.-M., Mattila, I., Hyötyläinen, T., Gopalacharyulu, P., Bounsaythip, C., Orešič, M., and Oksman-Caldentey, K.-M. (2011). Drug metabolome of the simvastatin formed by human intestinal microbiota in vitro. Mol. Biosyst. *7*, 437–446.

40. Đanić, M., Pavlović, N., Lazarević, S., Stanimirov, B., Vukmirović, S., Al-Salami, H., Mooranian, A., and Mikov, M. (2023). Bioaccumulation and biotransformation of simvastatin in probiotic bacteria: A step towards better understanding of drug-bile acids-microbiome interactions. Front. Pharmacol. *14*, 1111115.

41. Sprouffske, K., and Wagner, A. (2016). Growthcurver: an R package for obtaining interpretable metrics from microbial growth curves. BMC Bioinformatics *17*, 172.

42. Zou, L., Spanogiannopoulos, P., Pieper, L.M., Chien, H.-C., Cai, W., Khuri, N., Pottel, J., Vora, B., Ni, Z., Tsakalozou, E., et al. (2020). Bacterial metabolism rescues the inhibition of intestinal drug absorption by food and drug additives. Proc. Natl. Acad. Sci. U. S. A. *117*, 16009–16018.

43. Wishart, D.S., Feunang, Y.D., Guo, A.C., Lo, E.J., Marcu, A., Grant, J.R., Sajed, T., Johnson, D., Li, C., Sayeeda, Z., et al. (2018). DrugBank 5.0: a major update to the DrugBank database for 2018. Nucleic Acids Res. *46*, D1074–D1082.

44. Gohl, D.M., Vangay, P., Garbe, J., MacLean, A., Hauge, A., Becker, A., Gould, T.J., Clayton, J.B., Johnson, T.J., Hunter, R., et al. (2016). Systematic improvement of amplicon marker gene methods for increased accuracy in microbiome studies. Nat. Biotechnol. *34*, 942–949.

45. Bolyen, E., Rideout, J.R., Dillon, M.R., and Bokulich, N.A. (2019). Reproducible, interactive, scalable and extensible microbiome data science using QIIME 2. Nature.

46. Callahan, B.J., McMurdie, P.J., Rosen, M.J., Han, A.W., Johnson, A.J.A., and Holmes, S.P. (2016). DADA2: High-resolution sample inference from Illumina amplicon data. Nat. Methods *13*, 581–583.

47. Wang, Q., Garrity, G.M., Tiedje, J.M., and Cole, J.R. (2007). Naive Bayesian classifier for rapid assignment of rRNA sequences into the new bacterial taxonomy. Appl. Environ. Microbiol. *73*, 5261–5267.

48. Dixon, P. (2003). VEGAN, a package of R functions for community ecology. J. Veg. Sci.

49. McMurdie, P.J., and Holmes, S. (2013). phyloseq: an R package for reproducible interactive analysis and graphics of microbiome census data. PLoS One *8*, e61217.

50. Paradis, E., Claude, J., and Strimmer, K. (2004). APE: Analyses of Phylogenetics and Evolution in R language. Bioinformatics *20*, 289–290.

51. Fernandes, A.D., Macklaim, J.M., Linn, T.G., Reid, G., and Gloor, G.B. (2013). ANOVA-like differential expression (ALDEx) analysis for mixed population RNA-Seq. PLoS One *8*, e67019.

52. Fernandes, A.D., Reid, J.N., Macklaim, J.M., McMurrough, T.A., Edgell, D.R., and Gloor, G.B. (2014). Unifying the analysis of high-throughput sequencing datasets: characterizing RNA-seq, 16S rRNA gene sequencing and selective growth

experiments by compositional data analysis. Microbiome *2*, 15.

53. DeSantis, T.Z., Hugenholtz, P., Larsen, N., Rojas, M., Brodie, E.L., Keller, K., Huber, T., Dalevi, D., Hu, P., and Andersen, G.L. (2006). Greengenes, a chimera-checked 16S rRNA gene database and workbench compatible with ARB. Appl. Environ. Microbiol. *72*, 5069–5072.

54. Okonechnikov, K., Golosova, O., Fursov, M., and UGENE team (2012). Unipro UGENE: a unified bioinformatics toolkit. Bioinformatics *28*, 1166–1167.

55. Edgar, R.C. (2004). MUSCLE: multiple sequence alignment with high accuracy and high throughput. Nucleic Acids Res. *32*, 1792–1797.

56. Guindon, S., Dufayard, J.-F., Lefort, V., Anisimova, M., Hordijk, W., and Gascuel, O. (2010). New algorithms and methods to estimate maximum-likelihood phylogenies: assessing the performance of PhyML 3.0. Syst. Biol. *59*, 307–321.

57. Yu, G., Lam, T.T.-Y., Zhu, H., and Guan, Y. (2018). Two Methods for Mapping and Visualizing Associated Data on Phylogeny Using Ggtree. Mol. Biol. Evol. *35*, 3041–3043.

58. Chen, S., Zhou, Y., Chen, Y., and Gu, J. (2018). fastp: an ultra-fast all-in-one FASTQ preprocessor. Bioinformatics *34*, i884–i890.

59. Langmead, B., and Salzberg, S.L. (2012). Fast gapped-read alignment with Bowtie 2. Nat. Methods *9*, 357–359.

60. Anders, S., Pyl, P.T., and Huber, W. (2014). HTSeq—a Python framework to work

with high-throughput sequencing data. Bioinformatics *31*, 166–169.

61. Love, M.I., Huber, W., and Anders, S. (2014). Moderated estimation of fold change and dispersion for RNA-seq data with DESeq2. Genome Biol. *15*, 550.

62. Kanehisa, M., Sato, Y., and Morishima, K. (2016). BlastKOALA and GhostKOALA: KEGG Tools for Functional Characterization of Genome and Metagenome Sequences. J. Mol. Biol. *428*, 726–731.

63. Yu, G., Wang, L.-G., Han, Y., and He, Q.-Y. (2012). clusterProfiler: an R package for comparing biological themes among gene clusters. OMICS *16*, 284–287.

64. Wickham, H. (2016). Data Analysis. In ggplot2: Elegant Graphics for Data Analysis, H. Wickham, ed. (Springer International Publishing), pp. 189–201.

65. Price, M.N., Wetmore, K.M., Waters, R.J., Callaghan, M., Ray, J., Liu, H., Kuehl, J.V., Melnyk, R.A., Lamson, J.S., Suh, Y., et al. (2018). Mutant phenotypes for thousands of bacterial genes of unknown function. Nature *557*, 503–509.

66. Sinha, R., Stanley, G., Gulati, G.S., Ezran, C., Travaglini, K.J., Wei, E., Chan, C.K.F., Nabhan, A.N., Su, T., Morganti, R.M., et al. (2017). Index switching causes "spreading-of-signal" among multiplexed samples in Illumina HiSeq 4000 DNA sequencing. bioRxiv, 125724. 10.1101/125724.

67. Wetmore, K.M., Price, M.N., Waters, R.J., Lamson, J.S., He, J., Hoover, C.A., Blow, M.J., Bristow, J., Butland, G., Arkin, A.P., et al. (2015). Rapid quantification of mutant fitness in diverse bacteria by sequencing randomly bar-coded transposons. MBio *6*,

e00306–e00315.

68. Lechner, M., Findeiss, S., Steiner, L., Marz, M., Stadler, P.F., and Prohaska, S.J. (2011). Proteinortho: detection of (co-)orthologs in large-scale analysis. BMC Bioinformatics *12*, 124.

69. Zdobnov, E.M., and Apweiler, R. (2001). InterProScan--an integration platform for the signature-recognition methods in InterPro. Bioinformatics *17*, 847–848.

Chapter 3: Conclusion

In conclusion, our study's investigation into simvastatin's impact on human gut bacteria has uncovered significant insights into drug sensitivity mechanisms. Our analysis, spanning both individual strains and microbial communities, revealed the upregulation of drug-responsive genes related to membrane biogenesis and drug efflux, demonstrating the intricate strategies employed by bacteria to counter host-targeted drug effects.

This research lays a foundation for understanding the dynamic interplay between pharmaceutical agents and the human microbiota. As personalized medicine advances, our findings carry implications for tailoring interventions and optimizing treatment strategies based on individual patient profiles. By comprehending microbial responses to drugs, we are poised to enhance therapeutic outcomes, minimize unintended consequences, and navigate the complex landscape of drug-microbiota interactions in the pursuit of improved health and well-being.

Publishing Agreement

It is the policy of the University to encourage open access and broad distribution of all theses, dissertations, and manuscripts. The Graduate Division will facilitate the distribution of UCSF theses, dissertations, and manuscripts to the UCSF Library for open access and distribution. UCSF will make such theses, dissertations, and manuscripts accessible to the public and will take reasonable steps to preserve these works in perpetuity.

I hereby grant the non-exclusive, perpetual right to The Regents of the University of California to reproduce, publicly display, distribute, preserve, and publish copies of my thesis, dissertation, or manuscript in any form or media, now existing or later derived, including access online for teaching, research, and public service purposes.

DocuSigned by:
Veronica Escalante
BC8CE8FA681A40A...
Author Signature

8/29/2023
Date